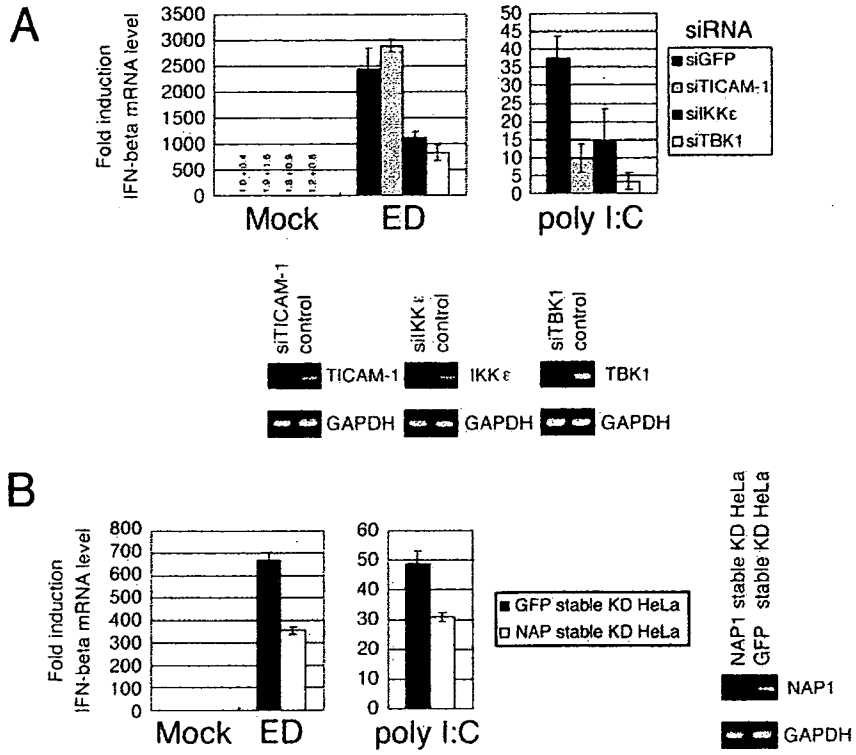

FIGURE 6. MV ED-mediated type I IFN induction depends on IKKε, TBK1, and NAP1, but not on TICAM-1. *A*, HeLa cells with TLR3 were transfected with siRNA targeted at TICAM-1, IKKε, or TBK1, and 72 h later cells were treated with Mock, ED, or poly I:C. Twenty-four hours later, RNA samples were recovered and mRNAs of IFN-β and β-actin were measured using RT- and Q-PCR. Normalization was performed. Relative fold induction against mock infection in GFP knockdown is shown. *B*, NAP1 or GFP stable knockdown HeLa cells were treated with Mock, ED (24 h), or poly I:C (2 h), and Q-PCR was performed as in *A*. Knockdown of each mRNA was confirmed by RT-PCR. Experiments were performed at least three times and representative results are shown.

the RIG-I- or MAVS-silenced cells were decreased by <20% of the control GFP siRNA cells. In the MDA5- or TBK1-silenced cells, the IFN-β mRNA levels were decreased by >50% of the control. In TICAM-1 silencing, however, no decrease of IFN-β mRNA was observed. When poly I:C was transfected, the cells efficiently induced IFN-β. The level of IFN-β mRNA was decreased in cells depleted of MDA5, MAVS, or TBK1 to ~25% of the GFP control (Fig. 8*B*). RIG-I silencing resulted in a 40% decrease of IFN-β induction in this setting. TICAM-1 silencing minimally affected the IFN-β mRNA level, suggesting that participation of TLR3 in IFN-β induction is negligible in HeLa cells. Taken together, these results strongly suggest that DI RNA induces IFN-β through the RIG-I/MDA5-MAVS pathway in the cytoplasm.

Similar experiments were performed using HeLa cells depleted of the factors in the IFN-inducing pathways and various MV strains. The rMV2A induced >100-fold less amounts of IFN-β mRNA compared with MV minireplicon RNA under the same conditions. ED and NV strains having DI RNA efficiently induced IFN-β mRNA early in infection of HeLa cells (Fig. 8*C*, *right panel*). The minute induction of IFN-β was suppressed by knockdown of RIG-I or MDA5 while MAVS silencing resulted in complete abrogation of IFN-β induction (Fig. 8*C*, *left panel*). Hence, in HeLa cells RIG-I and MDA5 share the IFN-β-inducing ability which totally relies on MAVS. Thus, the results again support the importance of DI RNA in IFN-β induction and involvement of the cytoplasmic RIG-I pathway in the induction of IFN-β in MV infection.

Discussion

MV is a negative-strand RNA virus which is believed to generate dsRNA for virus replication. However, a recent report suggested that influenza virus barely produces more than the detection limit

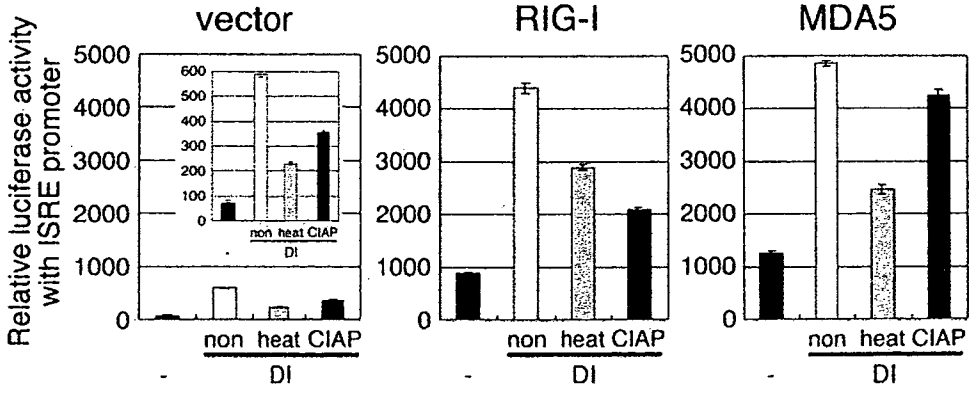

FIGURE 7. Phosphorylation and duplex structure of DI RNA differentially contribute to ISRE promoter activation via the cytoplasmic RNA sensors. HEK293 cells with pISRE-luc were prepared as in Fig. 3*B*. HEK cells were transfected with full-length RIG-I (*center panel*) or MDA5 (200 μg/5 × 10^5 cells; *right panel*) by polyfection. Empty vector was used as a control (*left panel*). Twenty-four hours later, cells were transfected with GFP minireplicon RNA (8 μg/ml) by Lipofectamine 2000. Six hours later, cells were harvested for reporter assay. Closed bars to the *left* in each panel represent reporter activity of cells with no stimuli, whereas DI means loading DI RNA. Non, Intact DI RNA; heat, heat-inactivated DI RNA; CIAP, CIAP-treated DI RNA. One of two similar experiments is shown.

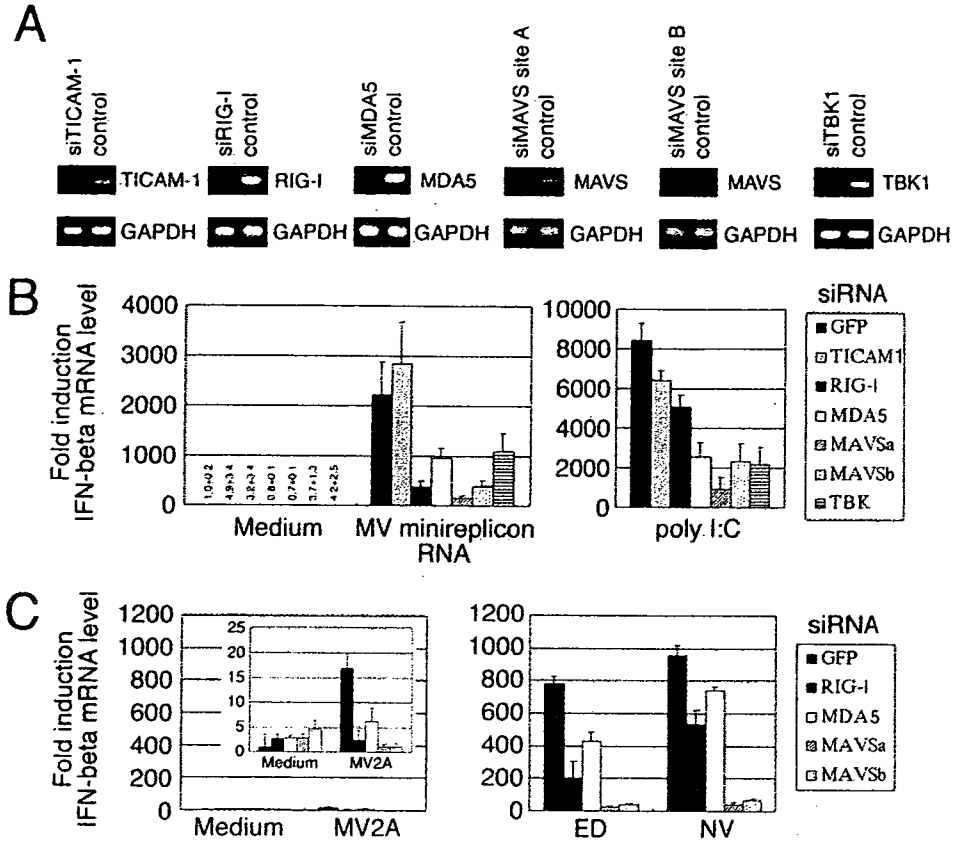

FIGURE 8. The route for type I IFN induction by MV minireplicon RNA and MV strains. HeLa cells were transfected with siRNA targeted at TICAM-1, RIG-I, MDA5, MAVS site A and B, or TBK1. *A*, Knockdown of each mRNA was confirmed by RT-PCR. *B*, Seventy-two hours after siRNA transfection, cells were transfected with MV minireplicon or poly I:C; or *C*, treated with Mock, MV2A (rMV ED strain), ED, or NV (ED and NV were laboratory adapted strains with 5′ copy-back DI). Twenty-four hours later, RNA samples were recovered and the mRNA levels of IFN-β, and β-actin were measured using RT- and Q-PCR. Normalization was performed. Relative fold induction against medium or mock infection in GFP knockdown is shown. The experiments were performed at least three times and representative results are shown.

of dsRNA by quantitative ELISA (45). Instead, triphosphate ssRNA activates RIG-I and induces IFN-α/IFN-β (45, 46). What is responsible for IFN induction in MV-infected cells has remained largely unknown. Here, we demonstrated that DI RNA participates in MV-mediated IRF-3 activation and type I IFN induction, which occur before virus replication (early phase). Infection with wild-type MV would produce triphosphate ssRNA but in the amount less than that required to activate RIG-I.

Naniche et al. and we previously reported that wild-type MV strains barely produce type I IFN during infection (16, 21). We demonstrated that an early induction of type I IFN by vaccine and laboratory adapted strains of MV depends on the coincidental DI RNA that resides in the virus particles. DI RNA rapidly induced type I IFNs, usually within 2 h after the virion fused with host cells. In contrast, effective viral RNA replication started 12 h p.i. Thus, in the context of DI RNA, IFN induction precedes viral replication to prevent the host cells from damage that accompanies viral replication. Furthermore, replication of the viral genome is retarded once DI RNA replicates in the same cells. At least, MV DI RNA inhibits viral amplification by two independent ways: IRF-3-mediated type I IFN induction and blockage of viral replication. Ultimately, virus strains containing DI RNA are attenuated in host cells by multiple means. Vaccine and laboratory adapted strains tend to possess DI RNA in addition to the genome within the particle. This DI RNA may act as a suppressor of virulence for initial step of virus infection.

We have learned from an earlier study on the MV substrains IC-B (84-01 B95a isolate) and IC-V (84-01 Vero isolate) (22) that the MV isolates from a single patient with acute measles gave rise to differential contents of DI RNA. The B95a-propagated substrain (IC-B) was highly pathogenic in experimental infection with cynomolgus monkeys while the Vero-propagated substrain (IC-V) had low pathogenicity in vivo. We have carefully propagated the MV strains IC-V and IC-B from their original lots and reproducibly detected DI RNA in the IC-V but not the IC-B stock. The MV substrains IC-B and IC-V derived from the same clinical material behave like wild-type and laboratory adapted strains, respectively. Their differential infectious properties appear to be rooted in the properties of the cells where the viruses were propagated. B95a cells can take up broad viral populations through the two orthologs of CD46 and CD150. Vero cells are known to have some deficiency in IFN induction (47). Adaptation of MV strains to Vero cells may foster amplification of DI RNA leading to the formation of DI RNA-containing virus particles that possess less toxicity by inducing type I IFN and blocking replication.

We performed PCR assay using the several original lots of the vaccine strains to detect the DI RNA. Unexpectedly, DI RNA was not detected in the CAM and AIK-C vaccine strains at least at the conditions used. It is possible that these two strains actually do not contain DI RNA or the primers chosen do not recognize the putative DI RNA sequences of these strains. As CAM and AIK-C have been established via plaque purification (48, 49), the original plaque may not have contained DI RNA. Alternatively, V or C proteins of these vaccine strains may be less functional for inhibition of IFNR-mediated amplification of type I IFN production (38, 50). The actual mechanism by which type I IFN is induced in CAM- or AIK-C-infected cells needs further investigation.

Previous studies suggested that the MV N-protein acts as a type I IFN inducer (36, 37). We found that N-protein minimally enhances IFN-α/IFN-β production and in conjunction with DI RNA far more up-regulates the IFN production than N protein alone (data not shown). Although the mechanism by which N protein potentiates DI RNA-mediated IFN production in the cells expressing the minireplicon RNA is intriguing, the possibility of interaction between the N protein and DI RNA has remained unaddressed. Anyhow, DI RNA rather than N protein is a potential

factor affecting the degree of IFN-α/IFN-β induction in the infected cells.

IFN-β was induced in human cells expressing either CD46 or CD150 in response to the infection by laboratory adapted strains. Laboratory and vaccine strains use CD46 in addition to CD150 as an entry receptor (51, 52). Wild-type strains do not enter the cells via CD46 (17, 18). As CD46 is ubiquitously expressed in human cells, including lymphocytes, mDCs, and macrophages, one can predict that CD46 is associated with IFN-β-inducing signals (53). However, irrespective of several experimental trials, we could not connect CD46 signaling with IFN-β induction (54). One possibility is that DI RNA production inadvertently coincides with CD46 receptor usage during MV strains passage in Vero cells. Recent reports indicate that CD46 functions as an immune modulator in lymphocytes and dendritic cells/macrophages (55, 56). The possibility that CD46 is involved in DI RNA-mediated immune responses should be revisited. Likewise, further studies on the properties of the RNA polymerase, nucleocapsid, and MV V protein in association with DI RNA production and receptor signal output in MV-infected cells will be required for further elucidation of measles-mediated immune modulation.

Previous reports suggested that the production of DI RNA is associated with viral-persistent infection (34). We considered whether DI RNA has an ability to regulate MV-persistent infection. DI RNA suppresses viral replication and reciprocally accelerates host IFN induction. Under the conditions where DI RNAs are being produced in cells, viruses are difficult to proliferate. Virus must change and adapt to the hostile environment for its survival and persistency of infection. Thus, DI RNA may be a factor to promote virus evolution and selective adaptation of viruses to host cells. However, the question still remains as to what factor is responsible for promoting initial viral persistency. If DI RNA plays a pivotal role in advancing viral adaptation, one could envisage it as a two-edged sword, decreasing pathogenicity and enhancing persistent infection. Additional study is needed to further explore this possibility.

After completing this study, we found two articles that were released relating to Sendai virus (SeV) DI RNA (57, 58). The level of IFN-β activation is shown to be proportional to that of SeV DI RNA replication and the viral V and C proteins are effective in blocking the copy-back DI RNA-induced activation of the IFN-β promoter (57). The other investigators state that SeV DI RNA is required for its robust mDC maturation (58). These investigators claim the importance of RIG-I in DI RNA-mediated IFN-β induction in SeV. In this study, we not only experimentally show that DI RNA activates IRF-3, but also further define the pathway taken by DI RNA to produce robust IFN-β. In MV ED studies, DI RNA, rather than the formation of the genomic dsRNA, causes IFN-β induction and mDC maturation in infected cells.

Note added in proof. Importance of 5′-phosphate-ended RNA in activation of RIG-I-mediated IFN response was also reported in MV infection by Plumet et al. (59).

Acknowledgments

We are grateful to Drs. A. Hirano (University of Washington, Seattle, WA), Y. Yanagi (Kyushu University, Hakata, Japan), F. Kobune (National Institutes of Health, Tokyo, Japan), T. Kimoto (Osaka Prefectural Public Health Institute, Osaka, Japan), A. Ueda (Osaka University, Osaka, Japan), K. Takeuchi (Tsukuba University, Ibaraki, Japan), N. Inoue, T. Akazawa (Osaka Medical Center for Cancer, Osaka, Japan), and M. Ayata (Osaka City University, Osaka, Japan) for providing cells, MV strains, and discussions. Thanks are also due to M. Kurita-Taniguchi (Osaka Medical Center for Cancer, Osaka, Japan) for technical assistance.

Disclosures

The authors have no financial conflict of interest.

References

1. Honda, K., A. Takaoka, and T. Taniguchi. 2006. Type I interferon gene induction by the interferon regulatory factor family of transcription factors. *Immunity* 25: 349–360.
2. Fitzgerald, K. A. 2006. Viral targeting of interferon regulatory factor-3 and type I interferon gene transcription. *Future Virol.* 1: 783–793.
3. Alexopoulou, L., A. C. Holt, R. Medzhitov, and R. A. Flavell. 2001. Recognition of double-stranded RNA and activation of NF-κB by Toll-like receptor 3. *Nature* 413: 732–738.
4. Matsumoto, M., S. Kikkawa, M. Kohase, K. Miyake, and T. Seya. 2002. Establishment of a monoclonal antibody against human Toll-like receptor 3 that blocks double-stranded RNA-mediated signaling. *Biochem. Biophys. Res. Commun.* 293: 1364–1369.
5. Heil, F., H. Hemmi, H. Hochrein, F. Ampenberger, C. Kirschning, S. Akira, G. Lipford, H. Wagner, and S. Bauer. 2004. Species-specific recognition of single-stranded RNA via Toll-like receptor 7 and 8. *Science* 303: 1526–1529.
6. Diebold, S. S., T. Kaisho, H. Hemmi, S. Akira, and C. Reis e Sousa. 2004. Innate antiviral responses by means of TLR7-mediated recognition of single-stranded RNA. *Science* 303: 1529–1531.
7. Hemmi, H., O. Takeuchi, T. Kawai, T. Kaisho, S. Sato, H. Sanjo, M. Matsumoto, K. Hoshino, H. Wagner, K. Takeda, and S. Akira. 2000. A Toll-like receptor recognizes bacterial DNA. *Nature* 408: 740–745.
8. Yang, Y. L., L. F. Reis, J. Pavlovic, A. Aguzzi, R. Schafer, A. Kumar, B. R. Williams, M. Aguet, and C. Weissmann. 1995. Deficient signaling in mice devoid of double-stranded RNA-dependent protein kinase. *EMBO J.* 14: 6095–6106.
9. Yoneyama, M., M. Kikuchi, T. Natsukawa, N. Shinobu, T. Imaizumi, M. Miyagishi, K. Taira, S. Akira, and T. Fujita. 2004. The RNA helicase RIG-I has an essential function in double-stranded RNA-induced innate antiviral responses. *Nat. Immunol.* 5: 730–737.
10. Andrejeva, J., K. S. Childs, D. F. Young, T. S. Carlos, N. Stock, S. Goodbourn, and R. E. Randall. 2004. The V proteins of paramyxoviruses bind the IFN-inducible RNA helicase, mda-5, and inhibit its activation of the IFN-β promoter. *Proc. Natl. Acad. Sci. USA* 101: 17264–17269.
11. Akazawa, T., T. Ebihara, M. Okuno, Y. Okuda, M. Shingai, K. Tsujimura, T. Takahashi, M. Ikawa, M. Okabe, N. Inoue, et al. 2007. Antitumor NK activation induced by the Toll-like receptor 3-TICAM-1 (TRIF) pathway in myeloid dendritic cells. *Proc. Natl. Acad. Sci. USA* 104: 252–257.
12. Biron, C. A., and L. Brossay. 2001. NK cells and NKT cells in innate defense against viral infections. *Curr. Opin. Immunol.* 13: 458–464.
13. Freigang, S., H. C. Probst, and M. van den Broek. 2005. DC infection promotes antiviral CTL priming: the "Winkelried" strategy. *Trends Immunol.* 26: 13–18.
14. Gotoh, B., T. Komatsu, K. Takeuchi, and J. Yokoo. 2002. Paramyxovirus strategies for evading the interferon response. *Rev. Med. Virol.* 12: 337–357.
15. Hengel, H., U. H. Koszinowski, and K. K. Conzelmann. 2005. Viruses know it all: new insights into IFN networks. *Trends Immunol.* 26: 396–401.
16. Naniche, D., A. Yeh, D. Eto, M. Manchester, R. M. Friedman, and M. B. A. Oldstone. 2000. Evasion of host defenses by measles virus: wild-type measles virus infection interferes with induction of α/β interferon production. *J. Virol.* 74: 7478–7484.
17. Lazzarini, R. A., J. D. Keene, and M. Schubert. 1981. The origins of defective interfering particles of the negative-strand RNA viruses. *Cell* 26: 145–154.
18. Tatsuo, H., N. Ono, K. Tanaka, and Y. Yanagi. 2000. SLAM (CDw150) is a cellular receptor for measles virus. *Nature* 406: 893–897.
19. Ono, N., H. Tatsuo, Y. Hidaka, T. Aoki, H. Minagawa, and Y. Yanagi. 2001. Measles viruses on throat swabs from measles patients use signaling lymphocytic activation molecule (CDw150) but not CD46 as a cellular receptor. *J. Virol.* 75: 4399–4401.
20. Seya, T., T. Hara, M. Matsumoto, and H. Akedo. 1990. Quantitative analysis of membrane cofactor protein (MCP) of complement: High expression of MCP on human leukemia cell lines, which is down-regulated during cell-differentiation. *J. Immunol.* 145: 238–245.
21. Murabayashi, N., M. Kurita-Taniguchi, M. Ayata, M. Matsumoto, H. Ogura, and T. Seya. 2002. Susceptibility of human dendritic cells (DCs) to measles virus (MV) depends on their activation stages in conjunction with the level of CDw150: role of Toll stimulators in DC maturation and MV amplification. *Microbes Infect.* 4: 785–794.
22. Kobune, F., H. Sakata, and A. Sugiura. 1990. Marmoset lymphoblastoid cells as a sensitive host for isolation of measles virus. *J. Virol.* 64: 700–705.
23. Ayata, M., T. Kimoto, K. Hayashi, T. Seto, R. Murata, and H. Ogura. 1998. Nucleotide sequences of the matrix protein gene of subacute sclerosing panencephalitis viruses compared with local contemporary isolates from patients with acute measles. *Virus Res.* 54: 107–115.
24. Kurita-Taniguchi, M., A. Fukui, K. Hazeki, A. Hirano, S. Tsuji, M. Matsumoto, M. Watanabe, S. Ueda, and T. Seya. 2000. Functional modulation of human macrophages through CD46 (measles virus receptor): production of IL-12 p40 and nitric oxide in association with recruitment of protein-tyrosine phosphatase SHP-1 to CD46. *J. Immunol.* 165: 5143–5152.
25. Kurita-Taniguchi, M., K. Hazeki, N. Murabayashi, A. Fukui, S. Tsuji, M. Matsumoto, K. Toyoshima, and T. Seya. 2002. Molecular assembly of CD46 with CD9, α_3-β_1 integrin and protein tyrosine phosphatase SHP-1 in human macrophages through differentiation by GM-CSF. *Mol. Immunol.* 38: 689–700.

26. Nishiguchi, M., M. Matsumoto, T. Takao, M. Hoshino, Y. Shimonishi, S. Tsuji, N. A. Begum, O. Takeuchi, S. Akira, K. Toyoshima, and T. Seya. 2001. Mycoplasma fermentans lipoprotein M161Ag-induced cell activation is mediated by Toll-like receptor 2: role of N-terminal hydrophobic portion in its multiple functions. *J. Immunol.* 166: 2610–2616.
27. Shingai, M., N. Inoue, T. Okuno, M. Okabe, T. Akazawa, Y. Miyamoto, M. Ayata, K. Honda, M. Kurita-Taniguchi, M. Matsumoto, et al. 2005. Wild-type measles virus infection in human CD46/CD150-transgenic mice: CD11c-positive dendritic cells establish systemic viral infection. *J. Immunol.* 175: 3252–3261.
28. Sasai, M., M. Shingai, K. Funami, M. Yoneyama, T. Fujita, M. Matsumoto, and T. Seya. 2006. NAK-associated protein 1 participates in both the TLR3 and the cytoplasmic pathways in type I IFN induction. *J. Immunol.* 177: 8676–8683.
29. Oshiumi, H., M. Matsumoto, K. Funami, T. Akazawa, and T. Seya. 2003. TICAM-1, an adaptor molecule that participates in Toll-like receptor 3-mediated interferon-β induction. *Nat. Immunol.* 4: 161–167.
30. Fitzgerald, K. A., S. M. McWhirter, K. L. Faia, D. C. Rowe, E. Latz, D. T. Golenbock, A. J. Coyle, S. M. Liao, and T. Maniatis. 2003. IKKε and TBK1 are essential components of the IRF3 signaling pathway. *Nat. Immunol.* 4: 491–496.
31. Seth, R. B., L. Sun, C. K. Ea, and Z. J. Chen. 2005. Identification and characterization of MAVS, a mitochondrial antiviral signaling protein that activates NF-κB and IRF 3. *Cell* 122: 669–682.
32. Takeda, M., K. Takeuchi, N. Miyajima, F. Kobune, Y. Ami, N. Nagata, Y. Suzaki, Y. Nagai, and M. Tashiro. 2000. Recovery of pathogenic measles virus from cloned cDNA. *J. Virol.* 74: 6643–6647.
33. Calain, P., J. Curran, D. Kolakofsky, and L. Roux. 1992. Molecular cloning of natural paramyxovirus copy-back defective interfering RNAs and their expression from DNA. *Virology* 191: 62–71.
34. Sidhu, M. S., J. Crowley, A. Lowenthal, D. Karcher, J. Menonna, S. Cook, S. Udem, and P. Dowling. 1994. Defective measles virus in human subacute sclerosing panencephalitis brain. *Virology* 202: 631–641.
35. Whistler, T., W. J. Bellini, and P. A. Rota. 1996. Generation of defective interfering particles by two vaccine strains of measles virus. *Virology* 220: 480–484.
36. Sharma, S., B. R. tenOever, N. Grandvaux, G. P. Zhou, R. Lin, and J. Hiscott. 2003. Triggering the interferon antiviral response through an IKK-related pathway. *Science* 300: 1148–1151.
37. tenOever, B. R., M. J. Servant, N. Grandvaux, R. Lin, and J. Hiscott. 2002. Recognition of the measles virus nucleocapsid as a mechanism of IRF-3 activation. *J. Virol.* 76: 3659–3669.
38. Takeuchi, K., S. I. Kadota, M. Takeda, N. Miyajima, and K. Nagata. 2003. Measles virus V protein blocks interferon (IFN)-α/β but not IFN-γ signaling by inhibiting STAT1 and STAT2 phosphorylation. *FEBS Lett.* 545: 177–182.
39. Matsumoto, M., K. Funami, M. Tanabe, H. Oshiumi, M. Shingai, Y. Seto, A. Yamamoto, and T. Seya. 2003. Subcellular localization of Toll-like receptor 3 in human dendritic cells. *J. Immunol.* 171: 3154–3162.
40. Yamamoto, M., S. Sato, K. Mori, K. Hoshino, O. Takeuchi, K. Takeda, and S. Akira. 2002. Cutting edge: a novel Toll/IL-1 receptor domain-containing adapter that preferentially activates the IFN-β promoter in the Toll-like receptor signaling. *J. Immunol.* 169: 6668–6672.
41. Meylan, E., J. Curran, K. Hofmann, D. Moradpour, M. Binder, R. Bartenschlager, and J. Tschopp. 2005. Cardif is an adaptor protein in the RIG-I antiviral pathway and is targeted by hepatitis C virus. *Nature* 437: 1167–1172.
42. Kawai, T., K. Takahashi, S. Sato, C. Coban, H. Kumar, H. Kato, K. J. Ishii, O. Takeuchi, and S. Akira. 2005. IPS-1, an adaptor triggering RIG-I- and Mda5-mediated type I interferon induction. *Nat. Immunol.* 6: 981–988.
43. Xu, L. G., Y. Y. Wang, K. J. Han, L. Y. Li, Z. Zhai, and H. B. Shu. 2005. VISA is an adapter protein required for virus-triggered IFN-β signaling. *Mol. Cell* 19: 727–740.
44. Sasai, M., M. Matsumoto, and T. Seya. 2006. The kinase complex responsible for IRF-3-mediated IFN-β production in myeloid dendritic cells (mDC). *J. Biochem.* 139: 171–175.
45. Hornung, V., J. Ellegast, S. Kim, K. Brzozka, A. Jung, H. Kato, H. Poeck, S. Akira, K. K. Conzelmann, M. Schlee, et al. 2006. 5′-Triphosphate RNA is the ligand for RIG-I. *Science* 314: 994–997.
46. Pichlmair, A., O. Schulz, C. P. Tan, T. I. Naslund, P. Liljestrom, F. Weber, and C. Reis e Sousa. 2006. RIG-I-mediated antiviral responses to single-stranded RNA bearing 5′-phosphates. *Science* 314: 997–1001.
47. Mosca, J. D., and P. M. Pitha. 1986. Transcriptional and posttranscriptional regulation of exogenous human β interferon gene in simian cells defective in interferon synthesis. *Mol. Cell. Biol.* 6: 2279–2283.
48. Makino, S., K. Sasaki, N. Nakamura, M. Nakagawa, and S. Nakajima. 1974. Studies on the modification of the live AIK measles vaccine. II. Development and evaluation of the live AIK-C measles vaccine. *Kitasato Arch. Exp. Med.* 47: 13–21.
49. Takaku, K., T. Sasada, T. Konobe, K. Onishi, and S. Ueda. 1970. Studies on further attenuated live measles vaccine. 3. Selection of less reactive variants of CAM measles vaccine virus. *Biken J.* 13: 163–168.
50. Nakatsu, Y., M. Takeda, S. Ohno, R. Koga, and Y. Yanagi. 2006. Translational inhibition and increased interferon induction in cells infected with C protein-deficient measles virus. *J. Virol.* 80: 11861–11867.
51. Yanagi, Y., M. Takeda, and S. Ohno. 2006. Measles virus: cellular receptors, tropism and pathogenesis. *J. Gen. Virol.* 87: 2767–2779.
52. Oldstone, M. B. A., D. Homann, H. Lewicki, and D. Stevenson. 2002. One, two, or three step: measles virus receptor dance. *Virology* 299: 162–163.
53. Katayama, Y., A. Hirano, and T. C. Wong. 2000. Human receptor for measles virus (CD46) enhances nitric oxide production and restricts virus replication in mouse macrophages by modulating production of α/β interferon. *J. Virol.* 74: 1252–1257.
54. Hirano, A., M. Kurita-Taniguchi, Y. Katayama, M. Matsumoto, T. C. Wong, and T. Seya. 2002. Isoform-specific ligation of human CD46 enhances interferon γ-dependent nitric oxide production in macrophages. *J. Biochem.* 132: 83–91.
55. Kemper, C., J. W. Verbsky, J. D. Price, and J. P. Atkinson. 2005. T-cell stimulation and regulation: with complements from CD46. *Immunol. Res.* 32: 31–43.
56. Oliaro, J., A. Pasam, N. J. Waterhouse, K. A. Browne, M. J. Ludford-Menting, J. A. Trapani, and S. M. Russell. 2006. Ligation of the cell surface receptor, CD46, alters T cell polarity and response to antigen presentation. *Proc. Natl. Acad. Sci. USA* 103: 18685–18690.
57. Strahle, L., D. Garcin, and D. Kolakofsky. 2006. Sendai virus defective-interfering genomes and the activation of interferon-β. *Virology* 351: 101–111.
58. Yount, J. S., T. A. Kraus, C. M. Horvath, T. M. Moran, and C. B. Lopez. 2006. A novel role for viral-defective interfering particles in enhancing dendritic cell maturation. *J. Immunol.* 177: 4503–4513.
59. Plumet, S., F. Herschke, J. M. Bourhis, H. Valentin, S. Longhi, and D. Gerlier. 2007. Cytosolic 5′-triphosphate ended viral leader transcript of measles virus as activator of the RIG-I-mediated interferon response. *PloS ONE* 2: e279.

NAK-Associated Protein 1 Participates in Both the TLR3 and the Cytoplasmic Pathways in Type I IFN Induction[1]

Miwa Sasai,*† Masashi Shingai,* Kenji Funami,* Mitsutoshi Yoneyama,‡ Takashi Fujita,‡ Misako Matsumoto,*†§ and Tsukasa Seya[2]*§

TLR3 and the cytoplasmic helicase family proteins (retinoic acid-inducible gene I (RIG-I) and melanoma differentiation-associated gene 5 (MDA5)) serve as dsRNA pattern-recognition receptors. In response to poly(I:C), a representative of dsRNA, and viral infection, they have been shown to activate the transcription factor IFN regulatory factor (IRF)-3, which in turn induces activation of the IFN-β promoter. RIG-I/MDA5 recognizes dsRNA in the cytoplasm, whereas TLR3 resides in the cell surface membrane or endosomes to engage in extracytoplasmic recognition of dsRNA. Recent reports suggest that TLR3 induces cellular responses in epithelial cells in response to respiratory syncytial virus (RSV). The modus for TLR3 activation by RSV, however, remains unresolved. By small interference RNA gene-silencing technology and human cell transfectants, we have revealed that knockdown of NAK-associated protein 1 (NAP1) leads to the down-regulation of IFN-β promoter activation >24 h after poly(I:C) or virus (RSV and vesicular stomatitis virus) treatment. NAP1 is located downstream of the adapter Toll-IL-1R homology domain-containing adapter molecule (TICAM)-1 (Toll/IL-1R domain-containing adapter-inducing IFN-β) in the TLR3 pathway, but TICAM-1 and TLR3 did not participate in the IRF-3 and IFN-β promoter activation by RSV infection. Virus-mediated activation of the IFN-β promoter was largely abrogated by the gene silencing of IFN-β promoter stimulator-1 (mitochondria antiviral signaling (MAVS), VISA, Cardif), the adapter of the RIG-I/MDA5 dsRNA-recognition proteins. In both the TLR and virus-mediated IFN-inducing pathways, IκB kinase-related kinase ε and TANK-binding kinase 1 participated in IFN-β induction. Thus, RSV as well as other viruses induces replication-mediated activation of the IFN-β promoter, which is intracellularly initiated by the RIG-I/MDA5 but not the TLR3 pathway. Both the cytoplasmic and TLR3-mediated dsRNA recognition pathways converge upon NAP1 for the activation of the IRF-3 and IFN-β promoter. *The Journal of Immunology,* **2006, 177: 8676–8683.**

The innate immune system serves as a primary defense against virus infection (1). It is accepted that retinoic acid-inducible gene I (RIG-I)[3] recognizes dsRNA in the cytoplasm, whereas TLR3 resides in the cell membrane to engage in extracellular recognition of dsRNA (2). Human TLR3 is expressed in airway epithelial cells and macrophages/myeloid dendritic cells (mDCs), which induce cytokines, IFN type I, and chemokines in viral infection (3–5). In response to poly(I:C) or viral dsRNA, RIG-I/MDA5 (melanoma differentiation associated gene 5) as well as TLR3 have been shown to activate the transcription factor IFN regulatory factor (IRF)-3, in turn inducing the activation of the IFN-β promoter (2). It remains unsettled whether TLR3 participates in viral infection-mediated IFN-β induction by detecting the extrinsic dsRNA originating from infected cells. Some reports have suggested that influenza virus, respiratory syncytial virus (RSV), and other viruses induce TLR3-mediated cellular responses in bronchial epithelial cells (5). Cytokine/chemokine responses are reported in influenza virus and RSV infection (3, 4, 6). In particular, RSV has been reported to serve as an inefficient inducer of type I IFNs (7), thereby being in part resistant to host antiviral immunity. The identification of the two pathways initiated by TLR3 and RIG-I, which involve IRF-3 activation followed by production of IFN-β, enabled an examination of the IFN response occurring in virus-infected cells (1).

TLR3 and RIG-I act as dsRNA-recognition pattern receptors, and are followed by adapter molecules named TICAM-1 (Toll-IL-1R homology domain-containing adapter molecule 1) (Toll/IL-1R domain-containing adapter-inducing IFN-β; TRIF) and IFN-β promoter stimulator (IPS)-1 (mitochondria antiviral signaling (MAVS)/VISA/Cardif), respectively, that indirectly link the common kinase complex IκB kinase-related kinase ε (IKKε) and TANK-binding kinase 1 (TBK1) (8–14). These kinases in turn activate IRF-3 and then the IFN-β promoter (15, 16). Thus, the two pathways must converge upstream of the kinase complex. However, the primary molecule responsible for connecting the two pathways to the kinases remains undetermined. The distinctive

*Department of Microbiology and Immunology, Hokkaido University Graduate School of Medicine, Kita-ku, Sapporo, Japan; †Department of Molecular Immunology, Nara Institute for Science and Technology, Ikoma, Nara, Japan; ‡Department of Molecular Genetics, Institute for Virus Research, Kyoto University, Kyoto, Japan; and §Department of Immunology, Osaka Medical Center for Cancer, Higashinari-ku, Osaka, Japan

Received for publication May 3, 2006. Accepted for publication September 20, 2006.

The costs of publication of this article were defrayed in part by the payment of page charges. This article must therefore be hereby marked *advertisement* in accordance with 18 U.S.C. Section 1734 solely to indicate this fact.

[1] This work was supported in part by Core Research for Engineering, Science, and Technology, Japan Science and Technology Corporation, by Grants-in-Aid from the Ministry of Education, Science, and Culture (Specified Project for Advanced Research) and the Hepatitis C Virus project in National Institutes of Health of Japan, and by the Naito Memorial Foundation, Uehara Memorial Foundation, Mitsubishi Foundation, and Osaka Community Foundation. M.Sa. is supported by fellowships from the Japanese Society for the Promotion of Science.

[2] Address correspondence and reprint requests to Dr. Tsukasa Seya, Department of Microbiology and Immunology, Graduate School of Medicine, Hokkaido University, Kita-ku, Sapporo 060-8638, Japan. E-mail address: seya-tu@pop.med.hokudai.ac.jp

[3] Abbreviations used in this paper: RIG-I, retinoic acid-inducible gene I; mDC, myeloid dendritic cell; MDA5, melanoma differentiation-associated gene 5; IRF, IFN regulatory factor; RSV, respiratory syncytial virus; TICAM-1, Toll-IL-1R homology domain-containing adapter molecule 1; TRIF, Toll/IL-1R domain-containing adapter-inducing IFN-β; IPS-1, IFN-β promoter stimulator 1; MAVS, mitochondria antiviral signaling; IKKε, IκB kinase-related kinase ε; TBK1, TANK-binding kinase 1; NAP1, NAK-associated protein 1; RNAi, RNA interference; pAb, polyclonal Ab; TIRAP, Toll/IL-1R domain-containing adaptor protein; CARD, caspase activation and recruitment domain; VSV, vesicular stomatitis virus; MOI, multiplicity of infection; siRNA, small interference RNA; IRES, internal ribosome entry site; sih, small interference hairpin-loop; Q-PCR, quantitative PCR; NAP1 DN, NAP1 dominant negative.

0022-1767/06/$02.00

role of the IFN-inducing pathways in mDC also remains to be elucidated.

NAK-associated protein 1 (NAP1) is initially characterized as an activator of IKK-related kinases and suggested to be involved in protection of cells from TNF-α-induced apoptosis (17). According to the study, the virus-activated kinases IKKε and TBK1 assemble in the regulatory subunit NAP1, and NAP1 facilitates activation of NF-κB by these kinases. In contrast, NAP1 coprecipitates with TICAM-1 by immunoprecipitation, suggesting the involvement of NAP1 in the TLR3-mediated IFN-inducing pathway (18). NAP1 forms a family with IKKγ and TANK, which recruit kinases to relay the signal for cellular responses (19). We previously showed that NAP1 but not TANK interacts with TICAM-1 (18). Using the RNA interference (RNAi) technology, we have searched for a molecule linking the TLR3 TICAM-1 pathway and the virus-mediated IFN-inducing pathway by infecting HeLa or HEK293 cells with viruses (including RSV, which reportedly derives TLR3 responses; Ref. 20). The results showed the gene silencing of NAP1 and the downstream kinases, but not TLR3 or TICAM-1, led to a decrease in IFN-β promoter activation. In the same system, exogenously added poly(I:C) required both TLR3 and TICAM-1 in addition to the NAP1-kinase complex for IFN-β induction. From these studies, we conclude that NAP1 essentially participates in both the TLR3 and RIG-I/MDA5-mediated IRF-3 activation pathways.

Materials and Methods

Cell culture and HeLa cell sublines

HeLa (a human cervical carcinoma cell line) cells were cultured in MEM with 2 mM L-glutamine and 10% heat-inactivated FCS (JRH Biosciences), and its subline Hep-2 cells (Japanese Cell Resource Bank) were cultured in DMEM (Invitrogen Life Technologies) with 10% FCS and antibiotics, 100 U/ml penicillin, and 100 μg/ml streptomycin (Invitrogen Life Technologies). In some experiments, we used alternative HeLa lines with stable siNAP1 vector for NAP1 silencing or siGFP vector for control. HEK293 cells (RIKEN) were cultured in DMEM as described previously (9).

Plasmid constructs and Ab

Poly(I:C) and anti-IRF-3 Ab were purchased from Amersham Biosciences and IBL. Rabbit-polyclonal Ab (pAb) against Flag (Sigma-Aldrich), against *myc* (Santa Cruz Biotechnology), and mouse mAb against *myc* (NeoMarkers or Covance) were purchased from the indicated suppliers. A mouse mAb against human NAP1 and a rabbit pAb against human RIG-I were prepared as reported previously (2, 17). The p-125 luc reporter was a gift from Dr. T. Taniguchi (Tokyo University, Tokyo, Japan) and contained the human IFN-β promoter region (−125 to +19). The Gal4-IRF-3, Gal4-DBD, and p55 UASG-Luc for IRF-3 activation, pEF-BOS-Flag-RIG-I, RIG-IN, MDA5, and MDA5N were described in Refs. 21 and 22). Expression vectors for NAP1-full, NAP1-DN, and del-NAP1 (NAP1 deleted of the TBK1 binding site; 158–270 aa) in pcDNA3.1 were prepared as described previously (17). Expression vector for IPS-1 (pEF-BOS-Flag-IPS1) was amplified by PCR using KIAA1271 (Kazusa DNA Research Institute) as a template. The dominant-negative form of Mal (Toll/IL-1R domain-containing adaptor protein; TIRAP) was prepared as described previously (23).

Immunoprecipitation

Methods for immunoprecipitation and immunoblotting were described previously (23). Briefly, HEK293 cells were transiently transfected with expression vectors in a 6-well plate using LipofectAMINE 2000 reagent (Invitrogen Life Technologies) and allowed to stand for 24 h. Cells were lysed and proteins were immunoprecipitated with anti-*myc* mAb (NeoMarkers). Immunoprecipitants were washed, resolved on SDS-PAGE (7.5 or 10% gel), and visualized by immunoblotting using the anti-Flag pAb or anti-*myc* pAb.

HeLa cells were used for detection of the endogenous NAP1-RIG-I interaction. Cells were cultured in DMEM/10% FCS with or without recombinant human IFN-β (1000 IU/ml) for 24 h. Cell lysates were immunoprecipitated by anti-NAP1 mAb or anti-mouse IgG Ab. Coimmunoprecipitation was detected by anti-RIG-I pAb.

Reporter gene assay

Activation of the IFN-β promoter was measured by reporter assay. HEK293 cells were transfected in 24-well plates using LipofectAMINE 2000 reagent with a p-125 luc (IFN-β) reporter plasmid together with the RIG-I, RIG-IN, MDA5, MDA5N or IPS-1, and NAP1 158–270 (NAP1-DN) plasmids. The properties of RIG-IN and MDA5N were published in a previous study (22). Briefly, the caspase activation and recruitment domain (CARD) of RIG-I (aa 1–284) acted as a constitutive active nature in the IFN-β induction. Luciferase activity was measured by the Dual-Luciferase assay kit (Promega). The luciferase activity of firefly was normalized to that of *Renilla*, and relative activation was determined. All experiments were performed in triplicate. Data were expressed as the means ± SD.

Assay for IRF-3 activation

Two methods, reporter assay (21) and native gel assay (24), were used to determine the degree of IRF-3 activation. In some experiments, cells were stimulated with medium alone, poly(I:C) (10 μg/ml), or vesicular stomatitis virus (VSV). In some experiments of reporter assay, cells were transfected with poly(I:C) using DEAE-dextran at 24 h posttransfection. Six hours later, cells were harvested to measure the expression of luciferase using the dual luciferase assay kit (Promega). Data were expressed as the means ± SD. In native assay, cells were lysed after 8 h VSV infection (multiplicity of infection (MOI) = 10). The protein level of each sample was measured by the Protein assay Kit (Bio-Rad) and normalized 20 μg/each lane. Extracts were separated on 7.5% native gel and immunoblotting with anti-IRF-3 Ab (24).

Confocal microscope analysis

HeLa cells (1.5×10^5 cells/well) were plated onto coverslips in a 24-well plate. After cells adhered onto coverslips, cells were transiently transfected with Flag-tagged IPS-1, *myc*-tagged NAP1, and/or *myc*-tagged TANK using LipofectAMINE reagent (Invitrogen Life Technologies). Twenty-four hours later, in a typical experiment, cells were treated with 250 nM Mito Tracker Red (Molecular Probes) for 1 h. Cells on coverslips were washed twice with PBS and fixed in 3% formaldehyde in PBS for 30 min. Cells were permeabilized with staining buffer (3% BSA in PBS) containing 0.5% saponin for 30 min at room temperature. After three washes with staining buffer, cells were incubated with primary Ab diluted in staining buffer for 1 h. Cells were extensively washed, and then were treated with Alexa Fluor 488 monoclonal or polyclonal, or Alexa Fluor 594 pAbs (Molecular Probes) as secondary Ab for 30 min. After three washes, coverslips with the cells were mounted onto slide glasses using 2.3% DABCO in PBS. Imaging of the cells was curried out using Olympus Fluoview laser scanning confocal microscopy (25).

Virus preparation and infection

Human RSV field-isolate strain (RSV2177) in subgroup B was propagated with Hep-2 cells (provided by Dr. K. Imai, Wakayama Prefectural Center, Wakayama, Japan) (26). The titer of RSV2177 was determined by 50% tissue culture infective dose using Hep-2 cells. This RSV strain derives type I IFN from Hep-2 cells >24 h postinfection (M. Shingai and T. Seya, unpublished observation). HeLa cells were infected with RSV for small interference RNA (siRNA) knockdown studies at MOI = 1 or 2.5.

VSV was propagated as described previously (27). In brief, VSV (Indiana strain) was propagated with L929 cells. The titration of VSV was determined by plaque assay using L929 cells. HeLa cells were infected with VSV at MOI = 10.

RNAi

RNAi knockdown by siRNA-containing vectors was performed regarding NAP1 as follows. A DsRed2 fragment derived from pDsRed2 (BD Clontech) was cloned into pBluescript II (Stratagene). To paste into the *Xho*I and *Spe*I site of the vector, the *Pst*I site of DsRed2 was replaced with CTGCAA by site-directed mutagenesis. Internal ribosome entry site (IRES) and puromycin resistance gene (Puro) fragments were amplified with an Expand High Fidelity PCR system (Roche Diagnostics) by using the following primer sets: AAACTAGTGCCCCTCTCCCTCCC and CTCACCATGGTTGTGGCCATATTATCATCGTGTTTTTCAAA, and AAACTCGAGTCCACCATGGGCACCGAGTACAAGCCC ACGGT and AAAACTAGTGCGGCCGCTCAGGCACCGGGCTT GCGGG, respectively. pME-Puro vector was generated by cloning of the *Xho*I-*Spe*I fragment of Puro and placing it between the *Xho*I and *Xba*I sites of the pME vector. The *Xho*I-*Spe*I fragment of DsRed2 and the *Spe*I-*Nco*I fragment of IRES were cloned into the pME-Puro vector. pH1′ vector was a gift from Drs. H. Hasuwa and M. Okabe (Osaka, Japan) (28). pH1′-DsRed-IRES-Puro was constructed by subcloning of

Table I. *Primer sets*

	Primer Set for RT-PCR	
	Forward	Reverse
RIG-I	5′-GATGGCAGGTGCAGAGAAA-3′	5′-GGAGTTAAAATGATGATGTC-3′
MDA5	5′-TCCAACTGCTGAACCTCCT-3′	5′-TGCCCATGTTGCTGTTATGT-3′
IPS-1	5′-TGCCGTTTGCTGAAGACAA-3′	5′-TTCGTCCGCGAGATCAACT-3′
	Primer Set for Q-PCR	
	Forward	Reverse
IFN-β	5′-CAACTTGCTTGGATTCCTACAAAG-3′	5′-TATTCAAGCCTCCCATTCAATTG-3′
β-Actin	5′-CCTGGCACCCAGCACAAT-3′	5′-GCCGATCCACACGGAGTACT-3′

the *Hin*dIII-*Kpn*I fragment of the pME-DsRed2-IRES-Puro vector into the pH1′ vector. Oligonucleotides were cloned into pH1 vector to express small interference hairpin-loop (sih)GFP and sihNAP1 (two sites) hairpins downstream of the human H1 RNA promoter as described previously (18, 28). 5′-AAGCTAATAGCTCGATTTGAAGA-3′ and 5′-AAGTGATAATATGCAGCATGCAT-3′ were the sequences targeted for sihNAP1-A and sihNAP1-B, respectively. The target sequence for sihGFP has been described earlier (28).

HeLa cells were transfected with pH1-GFP, pH1-NAP1-A, or pH1-NAP1-B (100 nM/4 × 10^5 cells) using PolyFect (Qiagen). Bulk cell populations in 1 mg/ml puromycin were selected from which single colonies were picked up for further analysis. To determine the efficiency of gene silencing, total RNA from each clone was isolated with RNeasy (Qiagen) and mRNA was estimated by RT-PCR. The primers used for PCR were GAPDH primers, and NAP1-F and NAP1-R for NAP1 (18).

The method for gene silencing using siRNA oligonucleotides was described previously (23). The sequences of the siRNA for TICAM-1 (9), TBK1, IKKε (15), RIG-I, and IPS-1 (MAVS) were reported previously (14). The target sequence for human MDA5 gene silencing is 5′-AAAUACCAUAAUGGAGCAAUA-3′. Knockdown was analyzed by RT-PCR.

Detection of human IFN-β mRNA

RT-PCR and quantitative PCR (Q-PCR) were performed as described previously (23). Briefly, human cells were transfected with gene silencing or dominant-negative-expressing vectors (100 nM/4 × 10^5 cells) 24 h before infection. Cells were then infected with RSV (MOI = 1–2.5). Twenty-four hours later, total RNA was extracted from cells with RNeasy mini kit (Qiagen) and cDNA was generated by M-MLV-reverse transcriptase

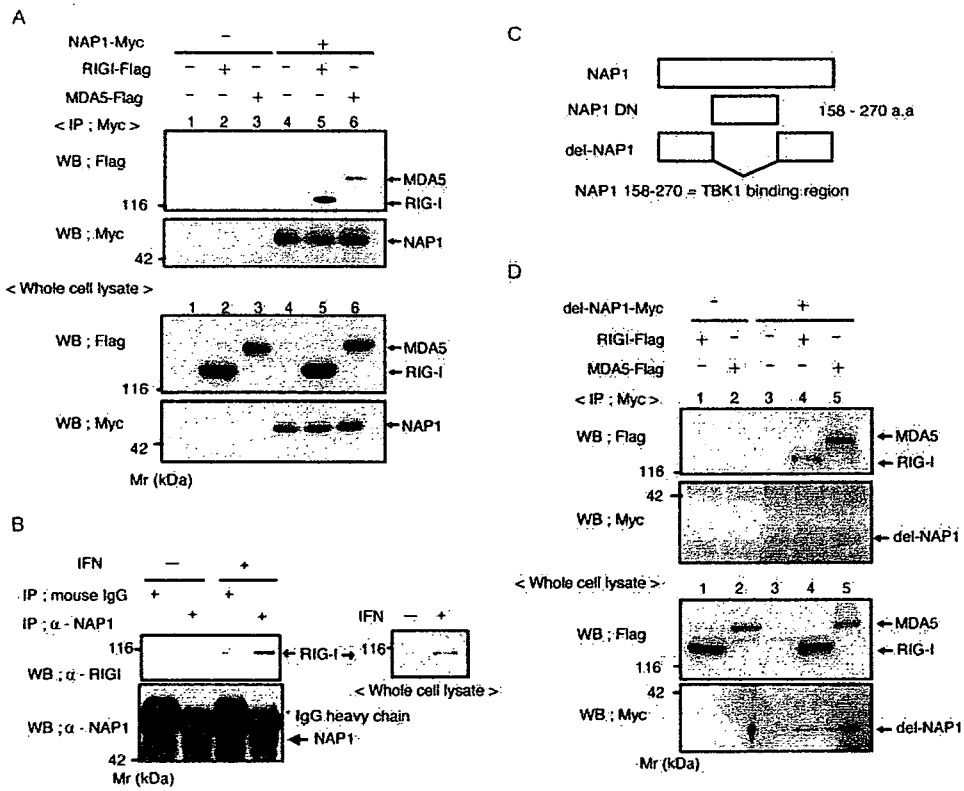

FIGURE 1. NAP1 interacts with RIG-I and MDA5. *A* and *D*, NAP1 associated with RIG-I and MDA5 in overexpression system. HEK293 cells were transiently transfected with expression vectors of NAP1 (*A*) or del-NAP1 (*D*) (*myc*-tagged), together with RIG-I or MDA5 (Flag-tagged) or empty vector, and allowed to stand for 24 h. Cells were then lysed and the lysates immunoprecipitated with anti-*myc* Ab. The precipitates were resolved on SDS-PAGE and transferred onto membrane. The blot was probed with anti-*myc* or anti-Flag Ab. Arrows indicate the positions of NAP1, RIG-I, and MDA5. M_r markers are shown to the *left*. *B*, Endogenous interaction between NAP1 and RIG-I. HeLa cells were pretreated with recombinant human IFN-β for 24 h. Extracts from IFN-treated or nontreated HeLa cells were immunoprecipitated with indicated Ab. The blot was probed with anti-RIG-I pAb or anti-NAP1 mAb. *, Indicates the mouse Ig H chain and arrow indicates the NAP1 or RIG-I band. Data are representative of three (*A* and *D*) or two (*B*) independent experiments. *C*, A schematic diagram of NAP1. The region of NAP1 158 to 270 aa was directly associated with TBK1.

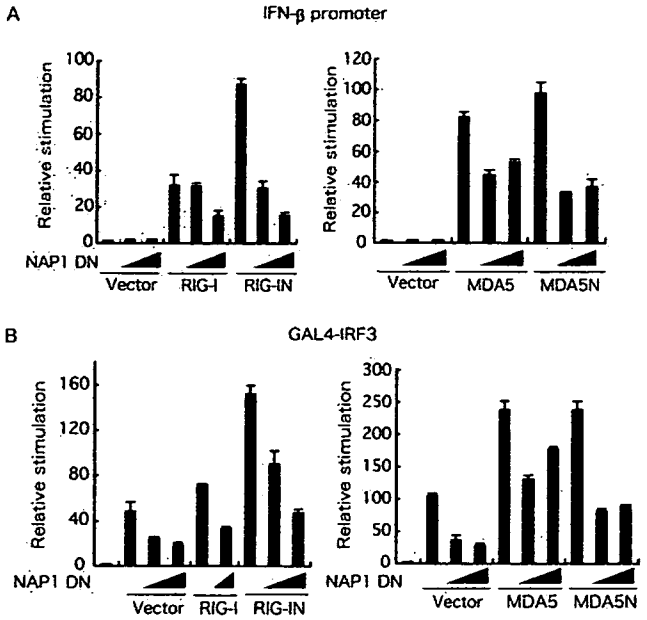

FIGURE 2. NAP1 participates in IRF-3, NF-κB, and IFN-β promoter activation via RIG-I and MDA5. *A*, HEK293 cells were transfected with the dominant-negative form of NAP1 158–270 (NAP1 DN) and expression vector RIG-I, RIG-IN (*left panel*), MDA5 or MDA5N together with the IFN-β promoter reporter plasmids. *B*, HEK293 cells were transiently transfected with p55-UAS$_G$Luc and pEF-GAL4/IRF-3, NAP1 DN, and empty vector, together with RIG-I, RIG-IN (*left panel*), MDA5 or MDA5N (*right panel*). After 24 h, luciferase reporter activity was measured and the relative firefly luciferase activity shown in normalized by *Renilla* luciferase activity. All data are representative of three independent experiments.

(Promega). cDNA was subjected to PCR using Ex-*Taq* DNA polymerase (Takara). For this study, previously described primer sets for IFN-β, NAP1, and TICAM-1 for silencing, and GAPDH or β-actin for internal control were used (9, 18, 23). Other primer sets for TBK1, IKKε, RIG-I, MDA5, and IPS-1 were described in Table I. Q-PCR was performed with iQ SYBER Green Super mix and iCycler iQ real-time PCR analyzing system (Bio-Rad). The primers used for IFN-β and β-actin on the Q-PCR were described in Table I. The copy number of IFN-β mRNA was normalized to β-actin mRNA, and relative fold induction of the medium to control was determined.

Results

NAP1 binds RIG-I and MDA5 in HEK293 transfectants

First, we tested whether RIG-I coprecipitates with NAP1 by immunoblotting using HEK293 cells. Cells were transfected with the indicated plasmids (Fig. 1*A*) and 24 h later solubilized with Nonidet P-40. NAP1 was immunoprecipitated with anti-*myc* Ab. Anti-Flag or anti-*myc* Ab was used as a probe for protein detection in immunoblotting. Flag-tagged RIG-I was shown to form a complex with *myc*-tagged NAP1 by analysis with SDS-PAGE followed by immunoblotting. RIG-I was identified together with NAP1 on the sheet, suggesting that RIG-I physically binds NAP1. Similar results were obtained with NAP1 and MDA5 (Fig. 1*A*). To confirm endogenous RIG-I physically binds NAP1, we used HeLa cells pretreated with IFN-β (Fig. 1*B*). RIG-I was efficiently induced in HeLa cells 24 h after IFN treatment (*inset* of Fig. 1*B*) and pulled down with NAP1 by immunoprecipitation using the mAb against NAP1.

NAP1 (158–270) (NAP1 DN; NAP1 dominant negative) can directly bind TBK1 and serve as a dominant-negative form in TICAM-1-mediated IFN signaling (17, 18). We tested whether NAP1 deleted this region (158–270) (del-NAP1) (Fig. 1*C*) could still interact with RIG-I and MDA5. Del-NAP1 preserves the ability to bind RIG-I and MDA5. Both RIG-I and MDA5 coprecipitated with this NAP deletion mutant (Fig. 1*D*), suggesting that the RIG-I/MDA5 binding site is mapped outside the TBK1 binding site. Because the large amount of NAP1 present in human cells prevents overexpression analysis, NAP1 DN was used for the following experiments as a dominant negative for the IFN pathway.

RIG-I and MDA5 participate in the NAP1-mediated signaling

RIG-I and MDA5 contain two CARDs. The CARDs of RIG-I recruits a CARD-containing adapter IPS-1. The CARD domains of RIG-I (RIG-IN) and MDA5 (MDA5N) have been used in addition

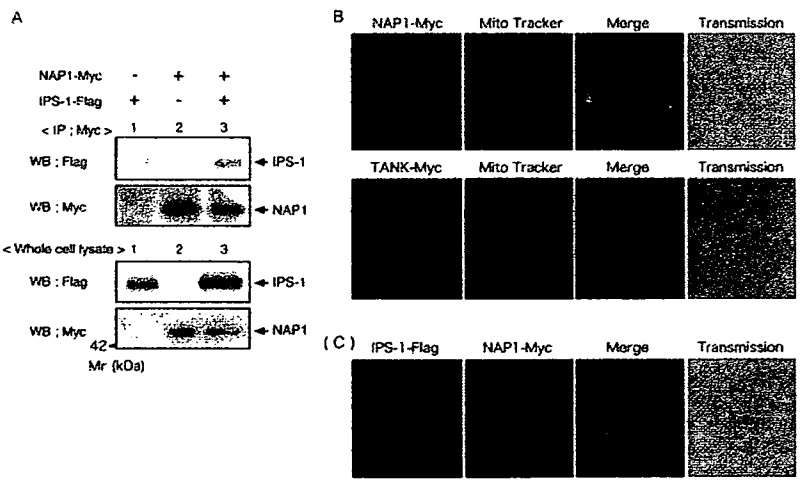

FIGURE 3. NAP1 colocalizes with IPS-1 in mitochondria. *A*, Minute physical interaction between NAP1 and IPS-1. HEK293 cells were transfected with *myc*-tagged NAP1 and flag-tagged IPS-1. After 24 h of transfection, cell extracts were immunoprecipitated by anti-*myc* mAb. The precipitates were resolved on SDS-PAGE and transferred onto membrane. The blot was probed with anti-*myc* or anti-Flag Ab. Arrows indicate the positions of NAP1 and IPS-1. M_r markers are shown to the *left*. *B*, NAP1 partially located around mitochondria. HeLa cells onto coverslips were transfected with NAP1 or TANK (*myc*-tagged). Twenty-four hours after transfection, cells were incubated with Mito Tracker Red for 1 h. *myc*-tagged NAP1 or TANK were stained with anti-*myc* mAb and imaged by confocal microscopy. The yellow staining in the overlay indicates colocalization of NAP1 and Mito Tracker. *C*, NAP1 colocalized with IPS-1. HeLa cells onto coverslips were transfected with IPS-1 (Flag-tagged) and NAP1 (*myc*-tagged). Twenty-four hours after transfection, cells were stained with anti-*myc* mAb and anti-Flag pAb and imaged by confocal microscopy. Data are representative of four (*A*) or three (*B*) independent experiments.

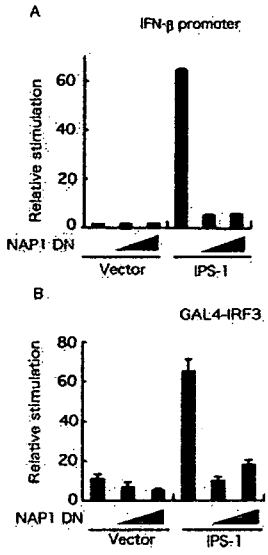

FIGURE 4. NAP1 DN-interfered IFN-β promoter and IRF-3 activation by IPS-1. *A*, HEK293 cells were transfected with the NAP1 DN and expression vector for IPS-1 together with the IFN-β promoter reporter plasmids. Cells were analyzed 24 h after transfection for promoter activity by a reporter gene assay. *B*, HEK293 cells were transiently transfected with p55-UAS$_G$Luc and pEF-GAL4/IRF3 and NAP1 DN together with empty vector or expression vector for IPS-1. Twenty-four hours after transfection, cells were collected and the promoter activation was measured by reporter gene assay. All data are representative of three independent experiments.

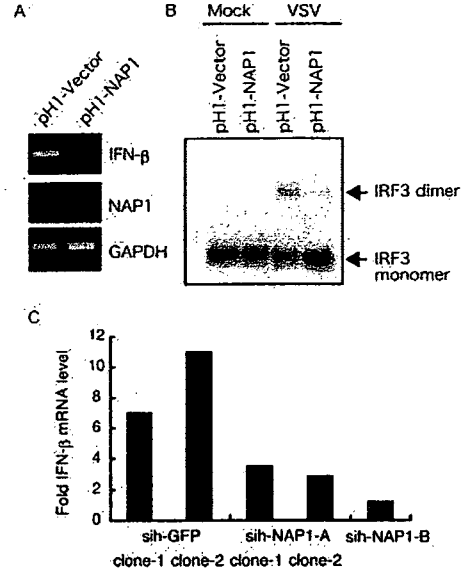

FIGURE 6. Implication of NAP1 in VSV infection-mediated IFN-β induction. *A*, NAP1 stable knockdown HeLa cells generate low levels of IFN-β mRNA in VSV infection. HeLa clones with the stably silencing NAP1 gene (data shown for pH1-NAP-A clone-1) or empty vector (control) were infected with VSV (MOI = 10) for 12 h. Total RNA was prepared, and RT-PCR analysis was performed with specific primers for NAP1, IFN-β, and GAPDH. *B*, NAP1-mediated IRF-3 activation in VSV infection. Stable NAP1-silenced HeLa cells (5.0×10^5 cells, pH1-NAP1-A clone-1) were infected with VSV (MOI = 10) for 8 h. Extracts were resolved by native gel electrophoresis. Dimerization of IRF-3 was detected by immunoblotting. *C*, VSV-mediated IFN-β induction is suppressed by NAP1 gene silencing. HeLa clones stably depleting NAP1 (clone-1 and clone-2 for sih-NAP1-A and a clone for sih-NAP1-B) or expressing siRNA against GFP (sih-GFP clone-1 and clone-2) were infected with VSV (MOI = 10) for 12 h. The IFN-β mRNA levels were determined with these cells by Q-PCR. Data are representative of two (*B*) or three (*C*) independent experiments.

to RIG-I and MDA5 for signaling studies. IFN promoter was activated in cells expressing RIG-IN and to a lesser extent in cells with full-length RIG-I (Fig. 2*A*). In this context, MDA5 and MDA5N elicited comparable activities. When increasing doses of NAP1 DN were added to the cells with RIG-I, MDA5, or their mutants, IFN-β promoter activation was prohibited by NAP1 DN

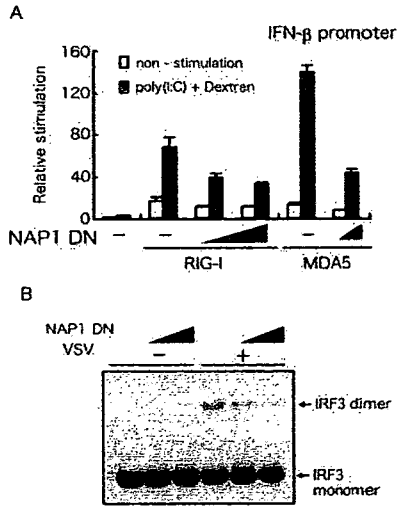

FIGURE 5. NAP1 DN inhibits IRF-3 activation. *A*, HEK293 cells were transfected with IFN-β promoter reporter plasmid together with the plasmids of RIG-I or MDA5 (100 ng) and NAP1 DN. Twenty-four hours after transfection, cells were transfected with dextran-only (nonstimulated) or poly(I:C)-mixed dextran for 6 h. *B*, HEK293 cells were transfected with NAP1 DN and cultured for 24 h. Cells were infected with VSV (MOI = 10) for 8 h. Extracts were subjected to native PAGE according to the reported method. Relative signal intensities of the dimer are shown below the lanes. These data are representative of three (*A*) or two (*B*) independent experiments.

in a dose-dependent manner (Fig. 2*A*). Using the Gal4-IRF-3 activation system, RIG-I- and MDA5-mediated IRF-3 activation was impaired in cells expressing NAP1 DN dose dependently (Fig. 2*B*). In the two systems, RIG-IN more potentially activated the promoters than intact RIG-I, whereas MDA5 and MDA5N exhibited similar tendencies (Fig. 2). Thus, the CARD domain of RIG-I induces activation of IRF-3 and IFN-β promoter, both of which are regulated by NAP1. It is notable, although consistent with a previous report (22), that the full-length MDA5 that contains the helicase domain exhibited high IFN-inducing activity compared with the case of RIG-I. A functional link between RIG-I/MDA5 and NAP1 is confirmed by this analysis in addition to the physical linkage.

Physical association between NAP1 and IPS-1

We next examined the ability of NAP1 to recruit IPS-1 in HEK293 cell transfectants. By simple immunoprecipitation analysis, NAP1 managed to coprecipitate with IPS-1 (Fig. 3*A*). Because IPS-1 resides in the mitochondrial membrane (14), we homogenized the transfectants and collected the mitochondria-rich fraction. Similar blotting results were obtained using this fraction (data not shown). Because NAP1 is a cytoplasmic protein, we investigated the localization of NAP1 using *myc*-tagged NAP1 expressed in HeLa cells by confocal microscopy. NAP1 was distributed in cytoplasm, particularly located around mitochondria (Fig. 3*B*, *upper panel*). In contrast, TANK, which is a structural homologue of NAP1, barely merged with mitochondrial marker (Fig. 3*B*, *lower panel*). To test

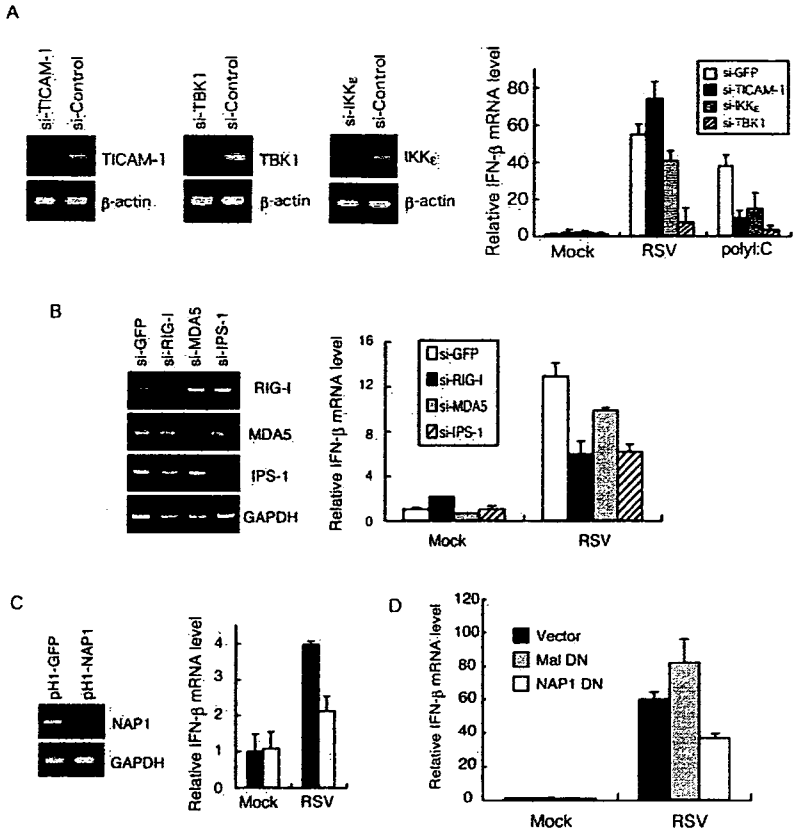

FIGURE 7. NAP1 is involved in IFN-β induction by RSV infection. *A*, HeLa cells were transfected with siRNA silencing for GFP, TICAM-1, IKKε, or TBK1. The indicated mRNAs levels shown after gene silencing were analyzed by RT-PCR. Cells were treated with RSV (MOI = 1 for 48 h) or poly(I:C) (10 μg/ml). Cells were lysed and mRNA levels of IFN-β were determined by Q-PCR. *B*, HeLa cells were transfected with siRNA silencing for GFP, RIG-I, MDA5, or IPS-1. The indicated mRNAs levels shown after gene silencing were analyzed by RT-PCR. Cells were treated with RSV (MOI = 2.5 for 48 h). *C*, HeLa stable clones of silencing NAP1 or GFP gene were infected with RSV (MOI = 1 for 48 h). The mRNAs levels of the cells are shown by RT-PCR. The mRNA levels of IFN-β were determined after RSV infection by Q-PCR. ■, GFP-silencing cells; □, NAP1-silencing cells. *D*, HEK293 cells were transiently transfected with the dominant-negative form of NAP1 or Mal/TIRAP. Twenty-four hours after transfection, cells were infected with RSV (MOI = 1 for 36 h). The mRNA levels of IFN-β in infected transfectants were measured as per *A*. Data are representative of two (*A–C*) or three (*D*) independent experiments.

the localization of NAP1 and IPS-1, Flag-tagged IPS-1 and *myc*-tagged NAP1 were expressed in HeLa cells, and merging analysis by confocal microscopy was performed. We confirmed that IPS-1 is the mitochondrial protein using our construct (data not shown). IPS-1 recruited NAP1 in the vicinity of the membrane (Fig. 3*C*). The results indicate that NAP1, at least in part, forms a complex with IPS-1 to relay the IRF-3-activating signal, although the reason why IPS-1 and NAP1 marginally coprecipitate with each other on immunoblotting remains unknown (Fig. 3*A*).

Concomitant functional analysis suggested that NAP1 DN blocks the IPS-1-mediated IFN-β promoter and IRF-3 activation (Fig. 4, *A* and *B*). Hence, there appear to be both physical and functional linkages between IPS-1 and NAP1. Thus, the results can be interpreted to most likely mean that the cytoplasmic (RIG-I/MDA5) and endosomal (TLR3) pathways converge on NAP1 to activate the IRF-3-activating kinases, leading to induction of IFN-β.

NAP1 DN and NAP1 decrease mediated inhibition of IFN induction by viral infection

Virus-mediated IRF-3 activation was examined with poly(I:C), VSV (Figs. 5 and 6), and RSV (Fig. 7), which are reported to activate cytoplasmic RIG-I and extracytoplasmic TLR3, respectively, to induce IFN promoter activation. Poly(I:C) is a reagent that activates the cytoplasmic IFN-inducing pathway in human cells in the presence of DEAE-dextran (Fig. 5*A*). HEK293 cells transfected with poly(I:C) using DEAE-dextran barely activated the IFN-β promoter in the reporter assay (*left-side* bars in Fig. 5*A*). When RIG-I and MDA5 were transfected into the cells before poly(I:C) stimulation, IFN-β promoter was activated by transfected poly(I:C), and NAP1-DN blocked those IFN-β promoter activation (Fig. 5*A*) and IRF-3 activation (data not shown). MDA5 prominently activated the IFN promoter compared with RIG-I, and this activity was efficiently impaired by co-transfection of NAP1 DN (Fig. 5*A*). Similar NAP1 DN-mediated suppression of IFN-β promoter activation was observed in cells without poly(I:C) (Fig. 5*A*), although the magnitude of the promoter activation was far less. A pervious study (29) demonstrated that VSV activates RIG-I in infected cells. VSV was subjected to the HEK293 cells instead of poly(I:C), and IRF-3 activation was tested in the reporter (data not shown) and native gel analyses (Fig. 5*B*). Under the conditions where IRF-3 is activated in response to VSV, NAP1 DN inhibited VSV-mediated IRF-3 activation in a dose-dependent manner (Fig. 5*B*). Thus, the results infer that RIG-I/MDA5 interacts with NAP1 in the virus-derived IFN-inducing pathway.

HeLa cell clones with stable gene silencing of NAP1 were established in an effort to confirm the essential role of NAP1 in virus-mediated IFN-β induction (Fig. 6*A*). IRF-3 dimer formation by VSV was apparently reduced in the NAP1-deficient cells (Fig. 6*B*). Concomitantly, the level of IFN-β mRNA was decreased in the NAP1-deficient cells (Fig. 6*C*). In this experiment, HeLa cell clones with the vector containing GFP siRNA were used as controls. Two NAP1-depleting clones of one target's site (site-A) and one depleting clone of another target site (site-B) showed similar low responses to VSV in IFN-β induction compared with the control (Fig. 6*C*), which excludes the possibility of artificial clonal effect. These results, together with the fact that VSV replication allows human cells to produce IFN-β in a RIG-I-dependent manner (29), suggest that NAP1 is indispensable to RIG-I-mediated IFN induction.

RSV is known to induce TLR3 responses in epithelial cells. RSV was used instead of VSV to confirm the effect on virus-activated IFN-β promoter activation in HeLa cells (Fig. 7). NAP1 as well as TICAM-1, IKKε, and TBK1 were silenced with siRNA, and the IFN-β mRNA levels were then measured in RSV-infected cells. Cells stimulated with poly(I:C) were used as control for the TICAM-1 pathway. As expected and consistent with previous reports, poly(I:C)-dependent IFN-β mRNA was found to be dependent on TICAM-1, IKKε, and TBK1 (Fig. 7*A*). Notably, TICAM-1 silencing had no

down-regulation effect on the IFN-β mRNA level, whereas IKKε and TBK1 were associated with RSV-mediated IFN induction (Fig. 7A). The IFN-β mRNA levels were evaluated 48 h after RSV infection in cells silencing of RIG-I, MDA5, or IPS-1. The IFN-β mRNA induction was most prominently impaired in cells depleted of RIG-I or IPS-1 (Fig. 7B). When NAP1 was silenced, 40% of the IFN-β mRNA level was reduced in the cells stimulated with poly(I:C) within 6 h (cells die during long-term incubation with poly(I:C)) (data not shown). In this system, RSV infection resulted in a 50% decrease of the NAP1-mediated IFN-β induction (Fig. 7C). To further confirm the involvement of NAP1 in the virus-mediated IFN-β-inducing pathway, we used the dominant-negative transfectants (Fig. 7D). No reduction of the IFN-β mRNA level was observed with the Mal/TIRAP dominant-negative-expressing HEK cells, whereas the IFN-β mRNA level was significantly decreased in cells expressing the NAP1 DN. Thus, RSV induces IFN-β independent of TICAM-1 but dependent on RIG-I, IPS-1, virus-activated kinases, and NAP1.

Discussion

In this study, we demonstrated that the CARD-helicase pattern-recognition receptors activate IRF-3 and the IFN promoter through NAP1, the regulatory subunit of the kinase complex IKKε and TBK1. The kinases IKKε and TBK1 are known to be virus-activated kinases (16) and are located downstream of TICAM-1 (also known as TRIF) (15). A previous study (18) revealed that NAP1 is also involved in a molecular complex containing TICAM-1. The N-terminal region out of the TIR domain of TICAM-1 participates in NAP1 recruitment. Thus, NAP1 works in the two different pathways for dsRNA-mediated IFN-β induction, TLR3/TLR4 followed by the TICAM-1 pathway and RIG-I/MDA5 followed by the IPS-1 pathway.

The results were consolidated with virus infection studies. RSV as well as VSV induces IFN-β in infected cells, and these viral IFN-inducing activities were blocked by NAP1 DN or siRNA, suggesting that NAP1 participates in virus-activated IRF-3 and IFN-β induction. NAP1 is implicated in the intracytoplasmic IFN-β-inducing signal in physical proximity to the molecular complex containing RIG-I and MDA5. Hence, NAP1 connects RNA sensor proteins (TLR3, RIG-I, and MDA5) and kinases to activate IRF-3. This scenario would be suitable to the findings of previous studies on IFN-β induction by cells with exogenously added poly(I:C) (18) and with replicated viruses (29).

NAP1 assembles IKKε and TBK1 to form a kinase complex (17). This kinase complex participates in activation of not only IRF-3 but also NF-κB. Actually, we have evidence that overexpression of RIG-I (particularly RIG-IN) or MDA5 in HEK cells results in activation of NF-κB and, under this situation, NAP1 DN blocks the NF-κB activation through RIG-I/MDA5 (data not shown). NF-κB activation through TNF-α receptors, however, revealed to involve two additional kinases, IKKα and IKKβ (30). Furthermore, two additional subunits, TANK and IKKγ, may affect the level of NF-κB activation (31). TLR4 as well as other TLRs principally activate NF-κB through IKKγ and a kinase complex with IKKα and IKKβ (32). In activation of NF-κB via NAP1, what combinations of the four kinases preferentially join the NAP1 protein complex still remains undetermined. Accordingly, molecular configuration of the kinase complex for activation of NF-κB remains to be defined downstream of IPS-1.

Using two species of viruses, VSV and RSV, RIG-I/MDA5 is evidently responsible for sensing viral infection to induce IFN-β. Previous reports have indicated that VSV stimulates the RIG-I pathway (33) and RSV induces TLR3 up-regulation and responses including cytokine/chemokine secretion in airway epithelial cells (4, 5, 20) Our gene silencing studies using siRNA (Fig. 7) and the RSV strain (an IFN-inducible strain) suggest that RIG-I is a key molecule in RSV-mediated IFN-β induction in HeLa cells. MDA5 or TLR3 minimally participates in RSV sensing, if any, in this in vitro study. VSV, a representative of the RIG-I-activating virus, confers a similar IFN-inducing profile to the RSV strain.

Hence, the involvement of TLR3 in the induction of type I IFN by RSV may reflect a secondary response resulting from TLR3 up-regulation by the initial production of IFN-β in virtue of RIG-I. We previously showed that NAP1 but not TANK interacts with TICAM-1 in the TLR3 pathway (18). Preferential recognition of RSV replication by RIG-I with no involvement of TLR3 and TICAM-1 appears to be additional evidence that NAP1 plays a major role downstream of RIG-I and outcome of viral infection. Because the results were obtained with HeLa and HEK293 cells in an acute-phase infection, this result should be confirmed with a cell line of bronchial epithelial cells and in vivo animal models.

However, it remains in question why IPS-1 only marginally coprecipitates with NAP1 in this study. According to the confocal analysis, NAP1 merges with IPS-1 on mitochondria. The discrepancy may be explained by the activation-induced mobility of IPS-1. IPS-1 overexpression leads to activation of the IFN-β promoter (Fig. 4A; Refs. 12, 13) and shows a merging profile with NAP1. A previous study (14) suggests that IPS-1 moves from a detergent-soluble to detergent-insoluble fraction in mitochondria following virus infection. The transposition of IPS-1 on the mitochondrial membrane may affect the dynamics of the cytoplasmic protein NAP1. So far, we have not yet established the system to see the molecular interaction between endogenous NAP1 and IPS-1. Maybe, the question lies in the artificial overexpression system. We favor the idea that IPS-1 forms a complex with NAP1, but the complex is fragile depending on the conditions where IPS-1 is disposed or solubilized from the mitochondrial membrane. Alternatively, NAP1 may only temporally bind IPS-1 on the mitochondrial membrane in initiating the pathway that activates IRF-3 in human cells. In this context, it is of interest to see the effect of viral infection on the molecular association between NAP1 and IPS-1.

Two further points remain to be discussed. First, our previous immunoprecipitation studies suggested that TICAM-1 forms a complex with NAP1 (18), whereas IPS-1 barely joins the complex containing TICAM-1 (data not shown). NAP1 coprecipitates with TICAM-1 irrespective of poly(I:C) activation of TLR3 (18). However, NAP1 does not merge with intrinsic TICAM-1 (data not shown), but with IPS-1 (Fig. 3C) largely around the mitochondria as shown by confocal analysis. The localization pattern of NAP1 is mysterious but may reflect the differential properties between TICAM-1 and IPS-1. Human cells mostly have a low level of TICAM-1 and a high level of IPS-1, and the level of TICAM-1 protein expression is usually suppressed because of its apoptosis-inducing properties (34). TICAM-1 undergoes protein modifications in response to poly(I:C) stimulation (M. Sasai and T. Seya, unpublished data), which may be a prerequisite for the recruitment of NAP1.

Secondly, RIG-I and MDA5 have been shown to be responsible for intracellular viral dsRNA recognition (33). They are cytoplasmic proteins of the CARD-helicase-containing family (22). RIG-I without a helicase domain (RIG-IN) acts as a constitutively active IFN inducer in transfected cells, whereas MDA5 expresses full IFN-inducing activity regardless of its helicase domain. The manner of ligand recognition may be somewhat different in each. Why RIG-I mainly participated in recognition of VSV/RSV infection is unknown. After completing this study, a report (29) was published showing that MDA5 preferentially recognizes poly(I:C) and the replicated RNAs of picornaviruses, whereas RIG-I recognizes transcribed dsRNAs of many RNA viruses. Although the report did not mention the natural ligand of MDA5, it offers evidence that MDA5 and RIG-I discriminate between the dsRNA structures

(29). Because RSV is a negative-strand RNA virus, it may hold a RNA structural motif inducing activation of RIG-I common to other negative-strand RNA viruses (35).

Pattern recognition molecules besides TLR3 and the CARD-helicase proteins are engaged in foreign RNA sensing in human cells. For example, TLR7 and TLR8 are expressed in human plasmacytoid DCs and mDCs, respectively (36). PKR is a receptor for dsRNA recognition (37). Generation of dsRNA may link to the pathway for inducing RNAi even in human cells. Why the host provides a variety of RNA pattern-recognition receptors and non-self RNA responses will be the issue to be clarified. Another point is that viral factors other than RNA have some host-immune-modulating functions. Measles nucleoproteins may modulate a Fcγ receptor-mediated immune response (38) and IRF-3 activation (39), which clearly occur independent of dsRNA or RNA replication. A recent report (40) suggests that negative-strand RNA viruses produce only undetectable amounts of dsRNA in infected cells. Although RIG-I is a key molecule in host protection against a number of RNA virus infections, other molecules and systems may be involved in host strategies against virus infection.

Acknowledgments

We are grateful to Drs. A. Ishii, T. Ebihara, and A. Matsuo in our laboratory for their critical discussions. Thanks are also due to Dr. K. Imai (Wakayama Prefectural Center, Wakayama, Japan) for providing us with RSV and to Drs. T. Fujita (Kyoto University, Kyoto, Japan), K. Miyake (Tokyo University, Tokyo, Japan), M. Nakanishi (the Nagoya City University, Nagoya, Japan), and T. Maniatis (Harvard Univeresity, Boston, MA) for providing their plasmids. Dr. Boru (Pacific Edit) reviewed this manuscript before submission.

Disclosures

The authors have no financial conflict of interest.

References

1. Akira, S., S. Uematsu, and O. Takeuchi. 2006. Pathogen recognition and innate immunity. *Cell* 124: 783–801.
2. Yoneyama, M., M. Kikuchi, T. Natsukawa, N. Shinobu, T. Imaizumi, M. Miyagishi, K. Taira, S. Akira, and T. Fujita. 2004. The RNA helicase RIG-I has an essential function in double-stranded RNA-induced innate antiviral responses. *Nat. Immunol.* 5: 730–737.
3. Matsumoto, M., K. Funami, M. Tanabe, H. Oshiumi, M. Shingai, Y. Seto, A. Yamamoto, and T. Seya. 2003. Subcellular localization of Toll-like receptor 3 in human dendritic cells. *J. Immunol.* 171: 3154–3162.
4. Rudd, B. D., J. J. Smit, R. A. Flavell, L. Alexopoulou, M. A. Schaller, A. Gruber, A. A. Berlin, and N. W. Lukacs. 2006. Deletion of TLR3 alters the pulmonary immune environment and mucus production during respiratory syncytial virus infection. *J. Immunol.* 176: 1937–1942.
5. Groskreutz, D. J., M. M. Monick, L. S. Powers, T. O. Yarovinsky, D. C. Look, and G. W. Hunninghake. 2006. Respiratory syncytial virus induces TLR3 protein and protein kinase R, leading to increased double-stranded RNA responsiveness in airway epithelial cells. *J. Immunol.* 176: 1733–1740.
6. Guillot, L., R. Le Goffic, S. Bloch, N. Escriou, S. Akira, M. Chignard, and M. Si-Tahar. 2005. Involvement of Toll-like receptor 3 in the immune response of lung epithelial cells to double-stranded RNA and influenza A virus. *J. Biol. Chem.* 280: 5571–5580.
7. Hall, C. B., K. R. Powell, N. E. MacDonald, C. L. Gala, M. E. Menegus, S. C. Suffin, and H. J. Cohen. 1986. Respiratory syncytial viral infection in children with compromised immune function. *N. Engl. J. Med.* 315: 77–81.
8. Yamamoto, M., S. Sato, H. Hemmi, K. Hoshino, T. Kaisho, H. Sanjo, O. Takeuchi, M. Sugiyama, M. Okabe, K. Takeda, and S. Akira. 2003. Role of adaptor TRIF in the MyD88-independent Toll-like receptor signaling pathway. *Science* 301: 640–643.
9. Oshiumi, H., M. Matsumoto, K. Funami, T. Akazawa, and T. Seya. 2003. TICAM-1, an adaptor molecule that participates in Toll-like receptor 3-mediated interferon-β induction. *Nat. Immunol.* 4: 161–167.
10. McWhirter, S. M., B. R. Tenoever, and T. Maniatis. 2005. Connecting mitochondria and innate immunity. *Cell* 122: 645–647.
11. Meylan, E., J. Curran, K. Hofmann, D. Moradpour, M. Binder, R. Bartenschlager, and J. Tschopp. 2005. Cardif is an adaptor protein in the RIG-I antiviral pathway and is targeted by hepatitis C virus. *Nature* 437: 1167–1172.
12. Kawai, T., K. Takahashi, S. Sato, C. Coban, H. Kumar, H. Kato, K. J. Ishii, O. Takeuchi, and S. Akira. 2005. IPS-1, an adaptor triggering RIG-I- and Mda5-mediated type I interferon induction. *Nat. Immunol.* 6: 981–988.
13. Xu, L. G., Y. Y. Wang, K. J. Han, L. Y. Li, Z. Zhai, and H. B. Shu. 2005. VISA is an adapter protein required for virus-triggered IFN-β signaling. *Mol. Cell* 19: 727–740.
14. Seth, R. B., L. Sun, C. K. Ea, and Z. J. Chen. 2005. Identification and characterization of MAVS, a mitochondrial antiviral signaling protein that activates NF-κB and IRF 3. *Cell* 122: 669–682.
15. Fitzgerald, K. A., S. M. McWhirter, K. L. Faia, D. C. Rowe, E. Latz, D. T. Golenbock, A. J. Coyle, S. M. Liao, and T. Maniatis. 2003. IKKϵ and TBK1 are essential components of the IRF3 signaling pathway. *Nat. Immunol.* 4: 491–496.
16. Sharma, S., B. R. tenOever, N. Grandvaux, G. P. Zhou, R. Lin, and J. Hiscott. 2003. Triggering the interferon antiviral response through an IKK-related pathway. *Science* 300: 1148–1151.
17. Fujita, F., Y. Taniguchi, T. Kato, Y. Narita, A. Furuya, T. Ogawa, H. Sakurai, T. Joh, M. Itoh, M. Delhase, et al. 2003. Identification of NAP1, a regulatory subunit of IκB kinase-related kinases that potentiates NF-κB signaling. *Mol. Cell. Biol.* 23: 7780–7793.
18. Sasai, M., H. Oshiumi, M. Matsumoto, N. Inoue, F. Fujita, M. Nakanishi, and T. Seya. 2005. Cutting Edge: NF-κB-activating kinase-associated protein 1 participates in TLR3/Toll-IL-1 homology domain-containing adapter molecule-1-mediated IFN regulatory factor 3 activation. *J. Immunol.* 174: 27–30.
19. Sasai, M., M. Matsumoto, and T. Seya. 2006. The kinase complex responsible for IRF-3-mediated IFN-β production in myeloid dendritic cells (mDC). *J. Biochem.* 139: 171–175.
20. Rudd, B. D., E. Burstein, C. S. Duckett, X. Li, and N. W. Lukacs. 2005. Differential role for TLR3 in respiratory syncytial virus-induced chemokine expression. *J. Virol.* 79: 3350–3357.
21. Yoneyama, M., W. Suhara, Y. Fukuhara, M. Fukuda, E. Nishida, and T. Fujita. 1998. Direct triggering of the type I interferon system by virus infection: activation of a transcription factor complex containing IRF-3 and CBP/p300. *EMBO J.* 17: 1087–1095.
22. Yoneyama, M., M. Kikuchi, K. Matsumoto, T. Imaizumi, M. Miyagishi, K. Taira, E. Foy, Y. M. Loo, M. Gale, Jr., S. Akira, et al. 2005. Shared and unique functions of the DExD/H-box helicases RIG-I, MDA5, and LGP2 in antiviral innate immunity. *J. Immunol.* 175: 2851–2858.
23. Oshiumi, H., M. Sasai, K. Shida, T. Fujita, M. Matsumoto, and T. Seya. 2003. TIR-containing adapter molecule (TICAM)-2, a bridging adapter recruiting to Toll-like receptor 4 TICAM-1 that induces interferon-β. *J. Biol. Chem.* 278: 49751–49762.
24. Iwamura, T., M. Yoneyama, K. Yamaguchi, W. Suhara, W. Mori, K. Shiota, Y. Okabe, H. Namiki, and T. Fujita. 2001. Induction of IRF-3/-7 kinase and NF-κB in response to double-stranded RNA and virus infection: common and unique pathways. *Genes Cells* 6: 375–388.
25. Funami, K., M. Matsumoto, H. Oshiumi, T. Akazawa, A. Yamamoto, and T. Seya. 2004. The cytoplasmic 'linker region' in Toll-like receptor 3 controls receptor localization and signaling. *Int. Immunol.* 16: 1143–1154.
26. Murabayashi, N., M. Kurita-Taniguchi, M. Ayata, M. Matsumoto, H. Ogura, and T. Seya. 2002. Susceptibility of human dendritic cells (DCs) to measles virus (MV) depends on their activation stages in conjunction with the level of CDw150: role of Toll stimulators in DC maturation and MV amplification. *Microbes Infect.* 4: 785–794.
27. Spielhofer, P., T. Bachi, T. Fehr, G. Christiansen, R. Cattaneo, K. Kaelin, M. A. Billeter, and H. Y. Naim. 1998. Chimeric measles viruses with a foreign envelope. *J. Virol.* 72: 2150–2159.
28. Hasuwa, H., K. Kaseda, T. Einarsdottir, and M. Okabe. 2002. Small interfering RNA and gene silencing in transgenic mice and rats. *FEBS Lett.* 532: 227–230.
29. Kato, H., O. Takeuchi, S. Sato, M. Yoneyama, M. Yamamoto, K. Matsui, S. Uematsu, A. Jung, T. Kawai, K. J. Ishii, et al. 2006. Differential roles of MDA5 and RIG-I helicases in the recognition of RNA viruses. *Nature* 441: 101–105.
30. Peters, R. T., and T. Maniatis. 2001. A new family of IKK-related kinases may function as IκB kinase kinases. *Biochim. Biophys. Acta* 1471: M57–M62.
31. Rothe, M., J. Xiong, H. B. Shu, K. Williamson, A. Goddard, and D. V. Goeddel. 1996. I-TRAF is a novel TRAF-interacting protein that regulates TRAF-mediated signal transduction. *Proc. Natl. Acad. Sci. USA* 93: 8241–8246.
32. Akira, S., K. Takeda, and T. Kaisho. 2001. Toll-like receptors: critical proteins linking innate and acquired immunity. *Nat. Immunol.* 2: 675–680.
33. Kawai, T., and S. Akira. 2006. Innate immune recognition of viral infection. *Nat. Immunol.* 7: 131–137.
34. Han, K. J., X. Su, L. G. Xu, L. H. Bin, J. Zhang, and H. B. Shu. 2004. Mechanisms of TRIF-induced ISRE and NF-κB activation and apoptosis pathways. *J. Biol. Chem.* 279: 15652–15661.
35. Melchjorsen, J., S. B. Jensen, L. Malmgaard, S. B. Rasmussen, F. Weber, A. G. Bowie, S. Matikainen, and S. R. Paludan. 2005. Activation of innate defense against a paramyxovirus is mediated by RIG-I and TLR7 and TLR8 in a cell-type-specific manner. *J. Virol.* 79: 12944–12951.
36. Iwasaki, A., and R. Medzhitov. 2004. Toll-like receptor control of the adaptive immune responses. *Nat. Immunol.* 5: 987–995.
37. Mogensen, T. H., and S. R. Paludan. 2005. Reading the viral signature by Toll-like receptors and other pattern recognition receptors. *J. Mol. Med.* 83: 180–192.
38. Marie, J. C., F. Saltel, J. M. Escola, P. Jurdic, T. F. Wild, and B. Horvat. 2004. Cell surface delivery of the measles virus nucleoprotein: a viral strategy to induce immunosuppression. *J. Virol.* 78: 11952–11961.
39. tenOever, B. R., M. J. Servant, N. Grandvaux, R. Lin, and J. Hiscott. 2002. Recognition of the measles virus nucleocapsid as a mechanism of IRF-3 activation. *J. Virol.* 76: 3659–3669.
40. Weber, F., V. Wagner, S. B. Rasmussen, R. Hartmann, and S. R. Paludan. 2006. Double-stranded RNA is produced by positive-strand RNA viruses and DNA viruses but not in detectable amounts by negative-strand RNA viruses. *J. Virol.* 80: 5059–5064.

Lamprey TLRs with Properties Distinct from Those of the Variable Lymphocyte Receptors[1]

Akihiro Ishii,* Aya Matsuo,* Hirofumi Sawa,† Tadayuki Tsujita,[2]* Kyoko Shida,‡ Misako Matsumoto,*‡ and Tsukasa Seya[3]*‡

Fish express mammalian-type (M-type) TLRs consisting of leucine-rich repeats (LRRs) and Toll-IL-1R (TIR) homology domain for immunity, whereas invertebrates in deuterostomes appear to have no orthologs of M-type TLRs. *Lampetra japonica* (lamprey) belongs to the lowest class of vertebrates with little information about its TLRs. We have identified two cDNA sequences of putative TLRs in the lamprey (laTLRs) that contain LRRs and TIR domains. The two laTLRs were 56% homologous to each other, and their TIRs were similar to those of members of the human TLR2 subfamily, most likely orthologs of fish TLR14. We named them laTLR14a and laTLR14b. We raised a rabbit polyclonal Ab against laTLR14b and identified a 85-kDa protein in a human HEK293 transfectant by immunoblotting using the Ab. FACS, histochemical, and confocal analyses showed that laTLR14b is expressed intracellularly in lamprey gill cells and that the overexpressed protein resides in the endoplasmic reticulum of human and fish (medaka) cell lines. Because natural agonists of TLR14 remained unidentified, we made a chimera construct of extracellular CD4 and the cytoplasmic domain of laTLR14. The chimera molecule of laTLR14b, when expressed in HEK293 cells, elicited activation of NF-κB and, consequently, weak activation of the IFN-β promoter. laTLR14b mRNA was observed in various organs and leukocytes. This lamprey species expressed a variable lymphocyte receptor structurally independent of laTLR14 in leukocytes. Thus, the jawless vertebrate lamprey possesses two LRR-based recognition systems, the variable lymphocyte receptor and TLR, and the M-type TLRs are conserved across humans, fish, and lampreys. *The Journal of Immunology*, 2007, 178: 397–406.

The first line of host defense against pathogen invasion is assigned by the innate immune system. This system involves a number of microbe pattern recognition receptors such as complement receptors, lectins, and TLRs. TLRs have recently been identified as the main receptors for the recognition of microbe-specific pattern molecules (1). TLRs structurally consist of extracytoplasmic leucine-rich repeats (LRRs)[4] and an intracytoplasmic Toll-IL-1R (TIR) homology domain (2–4), similar to *Drosophila* Toll (5). The LRRs sense microbes and the TIR transmits a signal for infectious response. The results of vertebrate and invertebrate genome projects have suggested that the TLR pattern recognition system is conserved across mammalian groups and probably most vertebrate species (6). In contrast, some invertebrates, based on their genomes, have only a few TLR-like proteins, whereas others have >100 members of the TLR family that are structurally unlinked to those of mammals (7). Toll homologues in insects and worms are often related to developmental functions rather than immunity (7, 8). In deuterostomes, based on their genome information invertebrates harbor TLR-like proteins with no homology to human TLRs (huTLRs), whereas gnathostomes, including fishes, amphibians, reptiles, birds, and mammals, have orthologs of huTLRs (6), which we designated the mammalian-type (M-type) TLR system (9). It is becoming clear that M-type TLR family members are mostly related to microbial pattern recognition for immunity (10). Thus, species-specific development of TLR expansion appears to have independently occurred in each division of insects, deuterostome invertebrates, and jawed vertebrates, most of which happen to have a TLR repertoire consisting of multiple members of Toll or TLRs with differential functions (7, 8). It remains unclear whether jawless vertebrates possess the TLR system comparable to that in humans.

Jawed vertebrates generate a lymphocyte receptor repertoire of sufficient diversity to discriminate the antigenic component of any pathogen (11–13). In jawed vertebrates including mammals, lymphocytes recognize peptides mounted on APCs to induce clonal lymphocyte proliferation and activate effector cells, leading to elimination of the pathogen. The initiation of these adaptive immune responses is triggered by the preceding activation of TLR signaling in the APCs. The Ig domains are used for the molecular interactions in the acquired immune system in jawed vertebrates. In contrast, the surviving jawless fish (agnathans), lamprey and hagfish, have diverse lymphocyte Ag receptor genes encoding LRRs (12–14). These cell surface receptors are designated variable lymphocyte receptors (VLRs) (12). VLRs are GPI-anchored proteins retained on the cell surface

*Department of Microbiology and Immunology, Graduate School of Medicine, Hokkaido University, Sapporo, Japan; †Department of Pathology, Zoonosis Center, Hokkaido University, Sapporo Japan; and ‡Department of Immunology, Osaka Medical Center for Cancer and Cardiovascular Diseases, Osaka, Japan

Received for publication February 16, 2006. Accepted for publication October 17, 2006.

The costs of publication of this article were defrayed in part by the payment of page charges. This article must therefore be hereby marked *advertisement* in accordance with 18 U.S.C. Section 1734 solely to indicate this fact.

[1] This work was supported in part by Core Research for Engineering, Science and Technology, Japan Science and Technology Corporation and by Grants-in-Aid from the Ministry of Education, Science and Culture (Specified Project for Advanced Research) of Japan and by the Mitsubishi Foundation (to T.S.), the Takeda Foundation (to T.S.), and the Uehara Memorial Foundation (to M.M.).

[2] Current address: Exploratory Research for Advanced Technology, Japan Science and Technology Corporation, Laboratory of Molecular and Developmental Biology, University of Tsukuba, Tennoudai 1-1-1, Tsukuba 305-8577, Japan.

[3] Address correspondence and reprint requests to Dr. Tsukasa Seya, Department of Microbiology and Immunology, Graduate School of Medicine, Hokkaido University, Kita-ku, Sapporo 060-8638, Japan. E-mail address: seya-tu@pop.med.hokudai.ac.jp

[4] Abbreviations used in this paper: LRR, leucine-rich repeat; ER, endoplasmic reticulum; fgTLR, fugu TLR; huTLR, human TLR; laTLR, lamprey TLR; M-type, mammalian-type; poly(I:C), polyinosinic-polycytidylic acid; TIR, Toll/IL-1R (homology domain); TICAM, TIR domain-containing adaptor molecule; VLR, variable lymphocyte receptor.

membranes or released in the fluid phase like Abs (7). Although the Ag-presenting mechanism, including the machinery for Ag presentation, has not been elucidated in agnathans, recombinatorial mechanisms for the generation of anticipatory receptors thus evolved in both jawless and jawed vertebrates (7). However, the role of innate immunity in the triggering of the VLR response has not been elucidated.

In humans and mice, the TLR system with a multigene family has been characterized as a functional entity specifically recognizing microbial pattern molecules independently of the acquired system (15, 16). To investigate whether jawless fish possesses the TLR family with a functional profile similar to that in humans, we used *Lampetra japonica* (lamprey) to analyze the TLR system. We searched lamprey tissues and cDNA libraries for fish TLR orthologs and found that the lamprey harbors two isoforms of the TLR2 subfamily. One of them resides inside lamprey cells and serves to deliver signals to activate NF-κB and, to a lesser extent, type I IFN in human cells. These results together with their subcellular localization profiles in human and fish cells suggest that the lamprey expresses immune-related TLR orthologs independently of the VLR system.

Materials and Methods

Lampreys

Live lampreys were purchased from Ebetsu Gyokyo. Sectioned tissues of the lamprey were stored at −80°C until use. Whole blood of the lamprey was drained from the dorsal aorta using a syringe, immediately added to an equal volume of Percoll (Amersham Biosciences), and then centrifuged at 2000 rpm for 10 min at 4°C, and the buffy coat was harvested to prepare leukocytes as previously described (17).

Because the chromosomes in jawless fish cells are unstable (18), no cell line is yet available. In addition, jawless fish genome information is difficult to obtain. For these reasons, we used human and fish (medaka, *Oryzias latipes*) cells instead of lamprey cells for the analysis of lamprey proteins. Although the data have been only partially published, the signal pathways of fish TLRs can be principally reconciled in human cells (19).

Cloning of lamprey TLRs (laTLRs) and construction of their constitutive active forms

laTLR DNA fragments were amplified by PCR with degenerated primers from a cDNA library of lamprey embryo mRNA as previously described (20). The primers were designed on the basis of the conserved TIR domain of 200-bp regions of fugu TLR (fgTLR) 1, huTLR1, huTLR6, and huTLR10. 3′- and 5′-RACE followed by consecutive PCR allowed us to identify two distinct sequences of laTLR-like products. The expected sizes of the two cDNA fragments were obtained by the PCR (data not shown). Full-length cDNAs were extended by consecutive PCR and then the two distinct cDNAs of laTLRs were cloned into pEFBOS vector (named laTLR14a and laTLR14b; GenBank accession nos. AB109402 and AB109403, respectively). A FLAG tag was attached to the C terminus of the protein in this vector. N-terminal FLAG-tagged laTLR14b was constructed in a pCMV-FLAG vector (Sigma-Aldrich) as described previously (21).

To analyze the signaling pathway of the laTLRs, TIR domains of laTLR14 (TIR14a and TIR14b) were fused with the human CD4 extracellular domain and cloned into the pEFBOS vector as constitutive active forms (1, 22). Each DNA fragment was amplified by PCR, and the obtained products were digested by *Xho*I and *Bgl*II (CD4), *Bgl*II and *Not*I (TIR14a), and *Bam*HI and *Not*I (TIR14b). The digested DNA fragments of the TIR and the CD4 fragment were cloned into the pEFBOS vector. Sequences of the primers used are shown in Table I.

Abs, cells, and proteins

Anti-human CD4 Ab was purchased from BD Biosciences. Anti-FLAG mAb was purchased from Sigma-Aldrich.

Human HEK293 HeLa cells were obtained from the American Type Culture Collection. RK13 cells (derived from rabbit kidney) were obtained from the RIKEN Cell Bank. HEK293 and RK13 cells were cultured in DMEM containing 10% heat-inactivated FCS. The HeLa cells were cultured in MEM with 2 mM L-glutamine and 10% FCS. These cells were transfected with expression vectors. The medaka fish cell line OL-17 (23) was a gift from Dr. H. Mitani (Tokyo University, Tokyo, Japan). Cells were cultured in L15 medium containing 10 mM HEPES buffer (pH 7.5) with 20% FCS at 33°C.

Rabbit anti-laTLR14b polyclonal Ab was produced by the method established in our laboratory (24). Briefly, RK13 cells (1×10^7) were transiently transfected with a pFLAG CMV-His×6 with full-length laTLR14b construct using LipofectAMINE PLUS reagent (Invitrogen Life Technologies). After 48 h, transfected RK13 cells were collected in 10 mM EDTA-PBS, washed three times with PBS, and suspended in 0.5 ml of PBS. The RK13 cell suspensions were then mixed and emulsified with 0.6 ml of Freund's complete adjuvant (Difco) and used for the immunization of rabbits. Immunization was performed four times at 7-day intervals, and the rabbits were boosted 3 days before drawing blood. Titers of the anti-laTLR14b Ab were roughly estimated by immunoblotting with lines of cell lysate containing laTLR14b (data not shown). IgG was purified by precipitation with 33% ammonium sulfate, dialyzed against PBS, and stored at −80°C until use.

Reporter assay

HEK293 cells (1×10^6 cells/well) were transiently transfected in 6-well plates by using LipofectAMINE 2000 reagent (Invitrogen Life Technologies) with reporter plasmid p-125 luc (IFN-β promoter) or luciferase-linked E-selectin (ELAM) promoter (NF-κB, 1 μg) and an internal control vector (phRL-TK, 0.2 ng; Promega). The total amount of DNA used for transfection was kept constant at 4 μg by adding an empty vector. After 24 h, cells were harvested and added to 96-well plates (5×10^4 cells/well) and stimulated with PBS, 10 μg/ml *Staphylococcus aureus* peptidoglycan (Furuka-Chemie), 100 nM macrophage-activating lipopeptide-2 (Biologica), 100 ng/ml Pam3 (BioLinks), 100 ng/ml LPS (Difco), 10 μg/ml polyinosinic-polycytidylic acid (poly(I:C); Amersham Biosciences), 1 μg/ml *Vibrio anguillarum* flagellin (19), and 1/100 volume of sonicated *Clostridium sporogenes* and *Salmonella typhimurium* cell lysates (25). After 6 h, cells were lysed in lysis buffer (Promega) and assayed for firefly and *Renilla* luciferase activities. Firefly luciferase activity was normalized with that of *Renilla* and expressed as fold stimulation relative to the activity of vector-transfected cells or PBS-stimulated cells. In some experiments, HEK293 cells (2×10^5 cells/well) in 24-well plates were transfected with pEFBOS/human CD4-laTLR14b plasmid (0.2 μg), the reporter plasmid (0.2 μg), internal control vector (0.1 ng), and the indicated expression vectors with dominant negative adapters (0.4 μg). After 12 h, cells were lysed and assayed for reporter activity. The SD was calculated from three separate experiments, each performed in triplicate.

RNA preparation and RT-PCR analysis

Individual female lampreys were dissected and the skin, gills, heart, liver, gut (stomach and intestine), kidneys, muscle, eyes, and eggs were harvested. A section above the vertebral column (called marrow) was aspirated with a syringe. One hundred milligrams of each tissue was homogenized in 1 ml of TRIzol reagent (Invitrogen Life Technologies) using a Dounce-type glass homogenizer and then total RNA was extracted by the TRIzol RNA preparation method. Five hundred nanograms of total RNA was treated with RQ1 RNase-free DNase and reverse transcribed with Moloney murine leukemia virus reverse transcriptase and random primers. For amplification of laTLR14 fragments, PCR was performed by denaturation at 94°C for 5 min followed by 35 cycles of 94°C for 30 s, 60°C for 30 s, and extension at 72°C for 30 s. *L. japonica* VLR DNA fragments were also amplified similarly for 30 cycles. Ex-*Taq* polymerase (Takara) and the indicated primers were used for both reactions (Table I).

Gene analysis

Assembling and editing of the determined DNA sequences were performed with ATGC and GENETYX-MAC version 12.1 software (Software Development). The sequences of the predicted open reading frames and TIR domains were compared with other sequences in a homology search by the BLAST program (www.ncbi.nlm.nih.gov/BLAST/). TLR14 members of *Takifugu rubripes* (GenBank accession nos. AC156431 and AAW69369), *Danio rerio* (GenBank accession no. XP_687315), and *Xenopus tropicalis* (Department of Energy Joint Genome Institute identifiers 190020, 30694, 421728, and 421736) were identified in the BLAST database. Alignment of amino acid sequences and unrooted phylogenic analysis of TLRs were performed using the ClustalW program (www.ddbj.nig.ac.jp/search/clustalw-j.html). Functional domains of the proteins were predicted by the SMART program (http://smart.embl-heidelberg.de/).

Flow cytometry and immunoblotting

Transfected HEK293 cells were analyzed for protein expression by flow cytometry and immunoblotting. For flow cytometric analysis, cells were

Table I. *Primers used in this study*[a]

Name	Sequence	Object
TLR16101	GANTGGTGCCAYTAYGGAR	Lamprey TLR cloning
TLR101R1	GCNCKNARGTTGGGCCARAA	Lamprey TLR cloning
TLRb85FW	TTTGCGGCCGCGAAAAAATGTTGCTGCGGAGAC	Construction for FLAG-tagged TLRb
TLRb2469RVS	TTTGTCGACTTTAAACATAAGGGTTACGGATTG	Construction for FLAG-tagged TLRb
CA_CD4FW	TTTCTCGAGCCCACAATGAACCGGGGAGTCCC	Construction for constitutive active form
CA_CD4RVS	TTTAGATCTCACCGGGGTGGACC	Construction for constitutive active form
CA_TIRaFW	TTTGAGATCTGCGATCGGACTC	Construction for constitutive active form
CA_TIRaRVS	TTTGCGGCCGCTTACTTGTCATCGTCGTC	Construction for constitutive active form
CA_TIRbFW	TTTGGATCCATCTCCATGAGCGTTGGAA	Construction for constitutive active form
CA_TIRbRVS	TTTGCGGCCGCTTAAACATAAGGGTTACGG	Construction for constitutive active form
RTa-500FW	TCCTTGAGAGAGCTGTATCTGACG	RT-PCR
RTa-RVS	AGTCCGAGTCCATGTGGCTGTAGG	RT-PCR
RTb-1000FW	GATTTTCCACGTACCCATGACGTACC	RT-PCR
RTb-500FW	TACATTGCACCCGAGTTGTACTCC	RT-PCR
RTb-RVS	GTGGGCACCAGGGTGTTCTCCACC	RT-PCR
Actin-FW	TGCTACGTGGCGCTCGACTTCGAG	RT-PCR
Actin-RVS	CCTTCTGCATGCGGTCGGCGATGC	RT-PCR
VLR-FW	CCTGGTGCAAAGTGCGGTAG	RT-PCR
VLR-RVS	CGGACGGGGGTATTGGTACCAG	RT-PCR

[a] FW, Forward; RVS, reverse.

stained with anti-TLR14b Ab (250-fold diluted in PBS with 0.2% BSA) or anti-FLAG Ab (5 μg/ml), washed in PBS containing 0.2% BSA and 0.1% sodium azide, and then incubated with FITC-conjugated goat anti-mouse IgG (American Qualex). Cells were washed and fluorescence intensity was measured (FACSCalibur; BD Biosciences). For immunoblotting, various lamprey tissues were solubilized in lysis buffer (1% (v/v) Nonidet P-40, 0.14 M NaCl, 0.01 M EDTA, 0.02 M Tris-HCl (pH 7.4), 1 mg/ml iodoacetamide, and 1 mM PMSF) using a Dounce-type homogenizer. After incubation at 4°C for 30 min, each lysate was centrifuged at 15,000 rpm for 30 min at 4°C. The supernatants were collected and protein concentration was measured using a protein estimation kit (Bio-Rad). Equal amounts of total cellular protein from each lysate were resolved by SDS-PAGE (7.5% gel) and transferred to polyvinylidene difluoride membranes. The membranes were incubated with either anti-laTLR14b Ab (1,000-fold diluted in PBS with 0.02% Nonidet P-40) or anti-FLAG Ab (5 μg/ml), washed in PBS containing 0.02% Nonidet P-40, and tagged by HRP-linked goat anti-rabbit second Ab (BioSource International). Proteins reacting to the Ab were visualized using an ECL detection system (Amersham Bioscience).

Confocal microscope analysis

HeLa cells or OL-17 cells of the Hd-rR strain of medaka (23) (1.5×10^5 cells/well) were plated onto coverslips in a 24-well plate. Cells were then transiently transfected with vectors expressing FLAG-tagged proteins. At timed intervals, the adherent cells were fixed for 30 min with 3% formaldehyde in PBS and permeabilized with 0.5% saponin in 1% BSA and PBS for 30 min and then washed four times with PBS. After the cells had been soaked in 1% BSA and PBS, they were treated for 1 h at room temperature with 5 μg/ml mouse anti-FLAG Ab (Sigma-Aldrich). The cells were then washed with 1% BSA and PBS and treated for 30 min at room temperature with Alexa 488-conjugated goat anti-mouse IgG (Molecular Probes) (1/400) in PBS. To see subcellular localization of the FLAG-tagged laTLRs, cells were treated with anti-FLAG Ab and Alexa 488 as described above and simultaneously stained with organella marker Abs; that is, rabbit anti-calnexin Ab (StressGen Biotechnologies) as an endoplasmic reticulum (ER) marker (1/200) or rabbit anti-EEA1 Ab (Affinity BioReagents) as an early endosome marker (4 μg/ml) and then Alexa 568-labeled goat anti-rabbit IgG for staining. The Golgi apparatus was stained with Texas Red-conjugated wheat germ agglutinin (1/100; Molecular Probes) and F-actin was stained by Phalloidin (1/500; Sigma-Aldrich. For acidic organelle staining, cells were pretreated with Lysotracker (final concentration of 1 mM) for 1 h before fixation. The stained cells were visualized at ×60 magnification under a FLUOVIEW microscope (Olympus). Images were captured using the attached computer software FLUOVIEW (26).

OL-17 cells were transfected with vectors and analyzed similarly to HeLa cells except for the transfection conditions, which are described in a previous report (23).

Immunohistochemical analysis

Formalin-fixed and paraffin-embedded sections were deparaffinized with xylene and rehydrated through a graded ethanol series. For Ag retrieval, sections were immersed in citrate buffer (pH 6.0) and heated using a pressure cooker. Thereafter, sections were treated with normal serum to eliminate nonspecific binding of Abs and incubated with 0.3% H_2O_2 methanol to quench endogenous peroxidase activity. After treatment, sections were incubated with rabbit anti-laTLR14b Ab (1/1000) at 4°C overnight. After incubation with EnVison goat anti-rabbit HRP-labeled second Ab (Dako-Cytomation), immunoreaction products were visualized with 3,3′-diaminobenzidine tetrahydrochloride (27, 28).

Results

cDNA cloning of lamprey TLRs

Many trials for the molecular cloning of lamprey TLRs were made with cDNAs prepared from an embryo of *L. japonica*. PCR amplification was successful using the primer set TLR16101 and TLR101R1 (Table I), which yielded a 210-bp cDNA fragment. A set of degenerate PCR primers was designed from conserved sequences (Fig. 1*A*; open rectangle) based on a homology search for TLR2 of various species (9, 29–31).

The cDNA fragment we cloned contained two distinct sequences encoding putative LRRs similar to those in huTLR2. By using the RACE method, the two sequences were extended over the pME18S-containing lamprey cDNA libraries (20). Finally, we identified two nucleotide sequences with putative open reading frames of LRRs and the TIR. We have prepared mRNAs from individual lampreys coming up the Ishikari river every year. The presence of this message was confirmed with adult lamprey gill mRNAs by sequencing 12 independent RT-PCR amplicons.

Deduced amino acid sequences from the cDNAs were analyzed by SMART programs, and the amino acid sequences are shown in Fig. 1*A*. Some LRR motifs and one TIR domain were predicted to exist. A hydrophobicity plot suggested that laTLR14a and 14b proteins are type I membrane proteins with signal peptides. These structures are shown in the Fig. 1*B*. These findings suggest that *L. japonica* has proteins of a TLR-like structure.

The two cloned laTLRs were highly homologous to each other (56% amino acid identities) (Fig. 1*C*). Recent BLASTP homology search analysis revealed that the laTLRs are most similar to the *T. rubripes* (pufferfish) TLR14 (fgTLR14) in the BLASTP database (Fig. 1*C* and Table II). We named these novel LRR-containing lamprey proteins laTLR14a and laTLR14b. The laTLR14a cDNA consisted of 2,486 bp, including an incomplete polyadenylation signal and poly(A) tail. This encoded a predicted protein of 815 amino acids whereas the laTLR14b cDNA consisted of 2,510 bp,

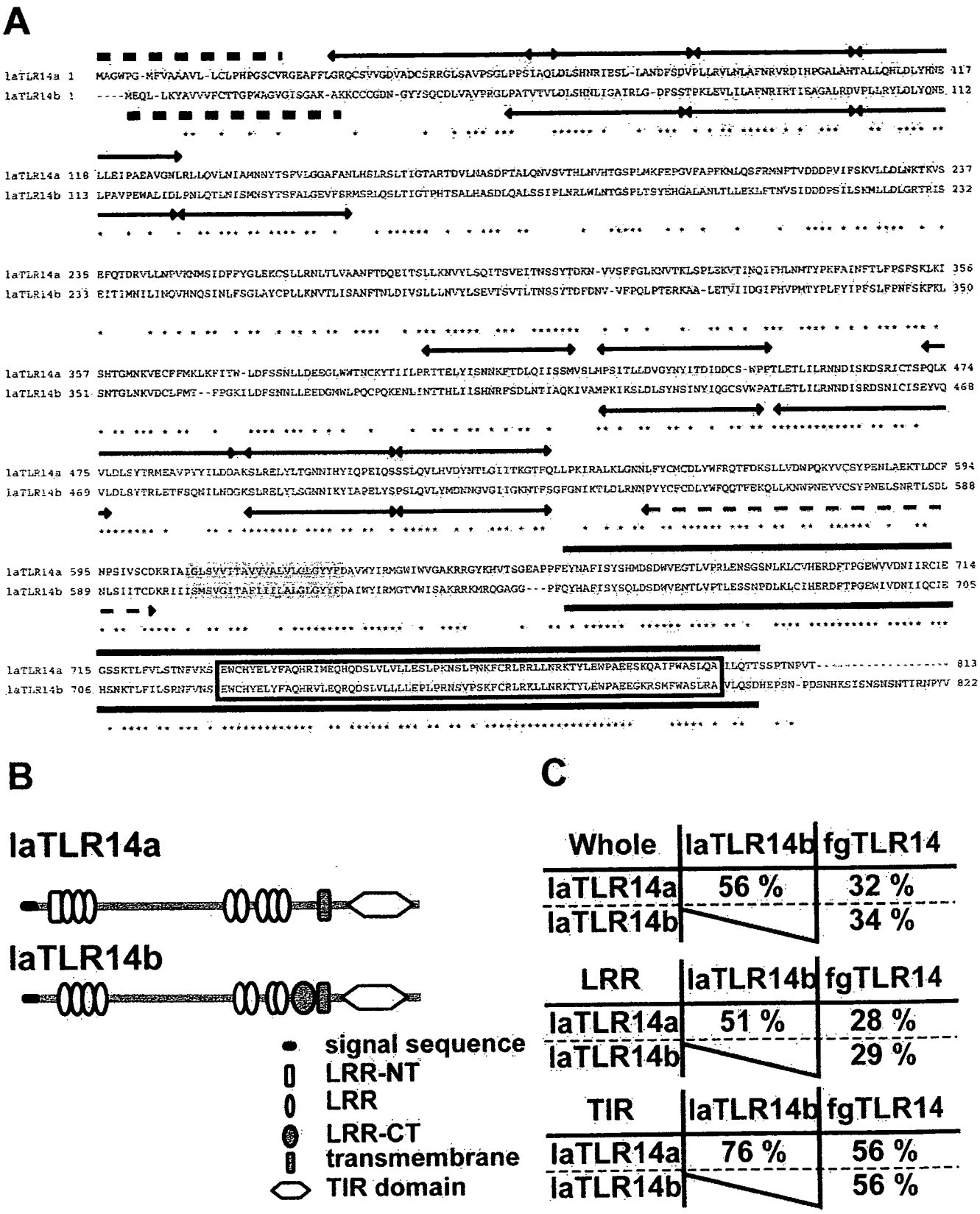

FIGURE 1. Amino acid alignment of cloned lamprey TLRs. *A*, Predicted amino acid sequences deduced from laTLR14a and laTLR14b cDNAs are aligned. Identical residues are indicated by asterisks, and each functional domain identified by the SMART program is shown by arrows (LRR-NT and LRR), gray box (TM), dotted arrow (C-terminal flanking region), dotted line (signal peptides), and solid line (TIR). *B*, Models of the predicted domain structures of laTLR14a and 14b. The LRR-CT domain of laTLR14a was not identified by SMART analysis. *C*, Percentage homology between fugu TLR14 (fgTLR14) and laTLR14a/b. The LRR and TIR regions are separately compared in the two *bottom tables*.

Table II. *Amino acid identities between fugu and lamprey TLRs*[a]

fgTLR	1	2	3	5	7	8	9	14	21	22	23
laTLR14a	30	29	21	23	Low	Low	Low	**33**	Low	23	Low
LRR[b]	25	26	21	23	Low	Low	Low	**27**	Low	24	Low
TIR[c]	47	44	30	31	36	38	35	**56**	42	40	39
laTLR14b	30	29	22	24	Low	Low	Low	**34**	Low	24	Low
LRR	26	24	21	23	Low	Low	Low	**29**	Low	24	Low
TIR	50	46	27	29	36	39	34	**58**	42	42	40

[a] The values of identities are indicated as a percentage, and the highest values are shown by bold numbers. Low. Percentage of similarity is too low to determine.
[b] LRR domain of laTLR14.
[c] TIR domain of laTLR14.

encoding a predicted protein of 822 amino acids (Fig. 1*A*). laTLR14a consisted of one unique N-terminal LRR-like motif (named LRR-NT), seven typical LRR motifs, one unique C-terminal LRR motif (named LRR-CT), followed by a transmembrane domain and a TIR domain (Fig. 1*C*). TLR14b structurally resembled TLR14a except for the lack of LRR-NT sequence. The TIRs of laTLR14a/b are most similar to that of fgTLR14 (>50% of amino acid identities). However, laTLR14a and laTLR14b exhibited only 29–34% identity to fgTLR14 in overall similarity (data not shown). The LRR domains of laTLR14 were <30% homologous to those of the huTLR2 subfamily, huTLR1, 2 6, and 10, although their TIR domains were >50% homologous (Table II). Bootstrap probability analysis suggested that TLR14 evolved from M-type TLR2 (Fig. 2 and Ref. 17). It is possible that laTLR14s were derived from the ancestral M-type TLR2 before the lamprey separated from fish and that laTLR14a and 14b diverged more recently after the lamprey species diverged from fish (Fig. 2). Hence, we suggest that the agnathan lamprey has structural orthologs of the gnathostome TLR system.

Protein expression of laTLRs

Protein expression and subcellular localization of laTLRs were analyzed in human HEK293 cells. We used pEFBOS-FLAG vector, which has the elongation factor promoter. Proteins of laTLR14a and laTLR14b with FLAG (either C-terminal or N-terminal) were detected by immunoblotting, flow cytometry, and immunofluorescence staining. laTLR14b (C-terminal FLAG) gave a thick protein band of 85 kDa and a thin band of 105 kDa by immunoblotting using an anti-FLAG Ab (Fig. 3*A*). This two-band profile was reproducible on the blot by using an Ab against laTLR14b (Fig. 3*A*). Only the 85-kDa band was detected in the lane with laTLR14a (C-terminal) in the blot using anti-FLAG Ab (Fig. 3*A*). The laTLR14b protein could be detected with the anti-laTLR14b Ab as well as anti-FLAG Ab (Fig. 3*A*). The molecular mass of 85 kDa is consistent with those expected from the two cDNA sequences of laTLRs. The 105-kDa protein form may be generated through posttranslational modifications.

By using flow cytometry with an anti-FLAG Ab, HEK293 cells expressing N-terminal laTLR14a or 14b were analyzed. laTLR14a (data not shown) and laTLR14b (Fig. 3*B*) were not detected on the surface of the transfected HEK cells. The laTLR14b with C-terminal FLAG showed a similar result (data not shown). When the cells were permeabilized and probed with anti-FLAG Ab (Fig. 3*C*), laTLR14b (C-terminal FLAG) was detected in the M1-positive gate by flow cytometry. Ultimately, ~10% of the transfected HEK cells expressed laTLR14b inside the cells.

We next probed laTLR14b in lamprey cells with the Ab against laTLR14b. The lamprey gill specimen was immunohistochemically stained using the Ab against laTLR14b. Some of cells in the epithelium of the lamprey gill were laTLR14b-positive (Fig. 3*D*), although the signal of laTLR14b was not very strong. laTLR14b appeared to reside inside the cells, consistent with the results of ectopic expression studies on laTLR14.

To see the localization of laTLRs in organelles, cells overexpressing laTLR14a and 14b were analyzed by a confocal microscope (Fig. 4). Two cell lines of human and fish were used for laTLR14 localization analysis. In human HeLa cells, FLAG-tagged laTLR14a and 14b were merged with the ER marker calnexin (Fig. 4A, *upper rows*), but not with markers for the Golgi apparatus (Fig. 4*A*, *lower rows*), endosomes, lysosomes, and F-actin (data not shown). In medaka OL-17 cells, the majority of the laTLR14 populations were localized to the ER, although some of them were distributed in other organelles (Fig. 4B, *upper rows*) but not merged with the Golgi apparatus (Fig. 4*B*, *lower rows*). Thus, like TLR9 as reported previously (32), laTLR14a and 14b are largely localized to the ER and only partly moved to other organelles.

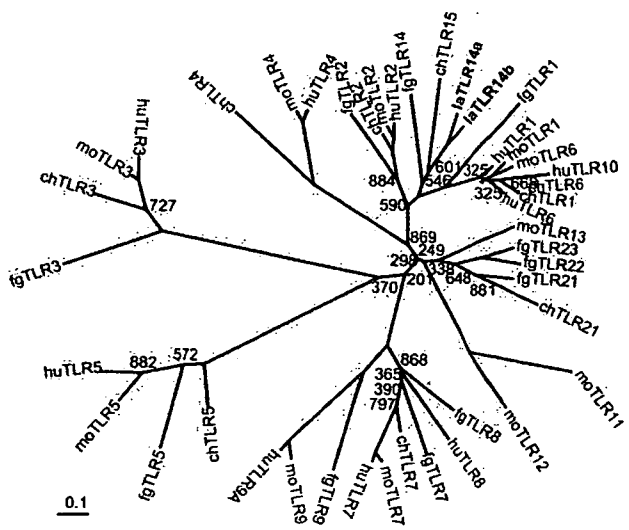

FIGURE 2. Phylogenetic tree for laTLR14a/b. Phylogenetic tree of puffer fish (fg), chicken (ch), mouse (mo), human (hu), and lamprey (la) TLRs. The amino acid sequences of the TIR domains were subjected to analysis. Bootstrap values (<900) are shown. Lamprey TLRs belonging to the TLR2 family are shown by bold characters.

Reporter assay for determination of promoter activation by laTLRs

Various ligands for huTLRs were tested to see whether they activate laTLR14a or 14b. The human HEK293 system with reporter genes was used because it can detect signals of fish and lamprey TLRs (33) (A. Ishii and T. Seya, unpublished data). Macrophage-activating lipopeptide-2, Pam3, *S. aureus* peptidoglycan, poly(I:C), LPS, and flagellin failed to elicit laTLR14a/b activation in

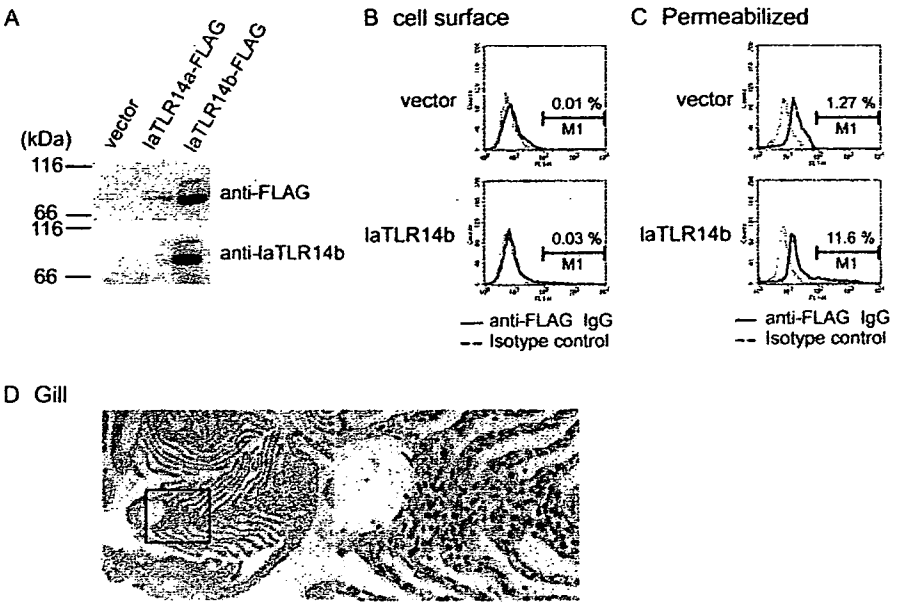

FIGURE 3. Protein expression analysis of laTLR14a/b. *A*, Immunoblotting. Plasmids containing C-terminal FLAG-tagged cDNAs of laTLR14a and laTLR14b were transfected into HEK293 cells. After 24 h, cells were solubilized and lysates were collected for immunoblotting. The blots were probed with an anti-FLAG Ab or an anti-laTLR14b Ab. The control contained only the vector. Molecular mass values are shown to the *left*. The minor bands above the laTLR14b protein may be a secondary product generated through modification. *B* and *C*, Flow cytometric analysis for surface-expressed and intracellular TLRs. HEK293 cells were transfected with vectors that allow the expression of an N-terminal FLAG-tagged laTLR14b protein. After 24 h, cells were treated first with anti-FLAG Ab and then with FITC-labeled goat anti-rabbit IgG Ab. Isotype-matched IgG was used as a control for the first Ab. laTLR14a was barely detectable with anti-FLAG Ab (data not shown). Intracellular TLRs were detected in permeabilized cells. Similar results were obtained using C-terminal-tagged constructs (data not shown). Percentages of cells in the M region are indicated. Three independent experiments gave similar results. A representative profile using the N-terminal tagged construct is given. *D*, Immunohistochemical staining of lamprey gills by an Ab against laTLR14b. The specimens were stained with an anti-laTLR14b Ab and a HRP-labeled second Ab. Nonimmune rabbit IgG was used as a negative control (not shown). *Left panel*, Original magnification, ×80; *right panel*, the marked region is enlarged (original magnification, ×400).

terms of NF-κB and the IFN-β promoter at the doses at which they activate huTLRs (data not shown). The reporters did not specifically respond to these reagents even with different transfection methods (data not shown). No significant increase of reporter was observed with any bacterial extract tested (*C. sporogenes and S. typhimurium*) for activation of laTLR14a/b (data not shown).

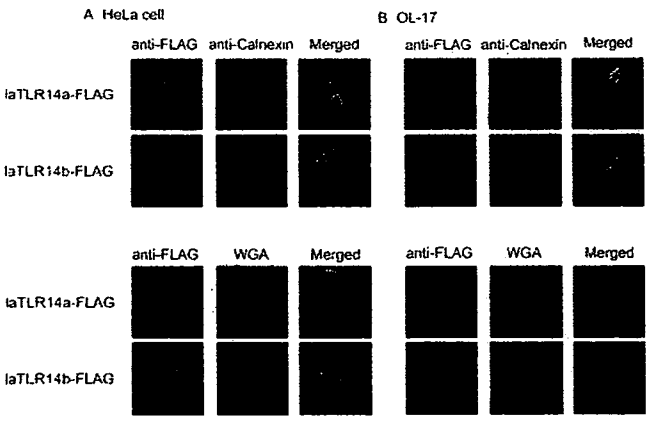

FIGURE 4. Subcellular localization of laTLR14a/b. HeLa cells (*A*) or medaka (Hd-rR) OL-17 cells (*B*) attached to coverslips were transfected with plasmid of laTLR14a or 14b (C-terminal FLAG-tagged). Twenty-four hours after transfection, cells were incubated with organelle markers for 1 h. FLAG-tagged proteins were stained with anti-FLAG Ab and imaged by confocal microscopy. The yellow staining in the overlay indicates co-localization of laTLR14. Examples for the colocalization analysis are shown for ER (calnexin) (*upper panels*) and Golgi (wheat-germ agglutinin (WGA)) (*bottom panels*). A predominant ER merging profile was observed in human HeLa cells as well as OL-17 fish cells (*B*), which were pretreated similarly to HeLa cells. Results of one of the three representative experiments is shown.

Functional analysis of the CD4-laTLR14b chimera protein

We next investigated whether the reporter is activated by the chimera construction with extracellular CD4 and intracellular laTLR14a or 14b by using HEK293 human reporter analysis. The Ig-like domains of human CD4 were ligated with the transmembrane and intracellular regions of laTLR14a or 14b (Fig. 5*A*). Flow cytometric analysis showed that ~3.6% of CD4-laTLR14a and 15% of CD4-laTLR14b were expressed on the surface of the transfected HEK293 cells (M1 region in Fig. 5*B*). Using the ELAM promoter and the p-125 luc promoter, we examined whether the chimera laTLR14a or laTLR14b elicits activation of the NF-κB and IFN-β promoter by CD4 dimerization. CD4-laTLR14b induced ELAM promoter-mediated NF-κB activation (Fig. 5*C*). The activation of NF-κB was suppressed by cotransfection of the MyD88 dominant negative form, suggesting that laTLR14b activates NF-κB via human MyD88. Human Mal and the Toll-IL-1R domain-containing adaptor molecule (TICAM)-1 appear not to be involved in the TLR14-mediated NF-κB activation pathway (Fig. 5*C*). CD4-laTLR14b only marginally induced IFN-β promoter activation, which was completely inhibited by cotransfection with MyD88 dominant negative in HEK cells (data not shown). The minute IFN-β promoter activation appears to be induced secondarily via MyD88 and NF-κB. Thus, laTLR14b is a signaling receptor for the activation of NF-κB in the human cell system.

Even though CD4-laTLR14a was slightly expressed on the surface of HEK transfectants, it barely induced signaling in response to CD4 dimerization (data not shown).

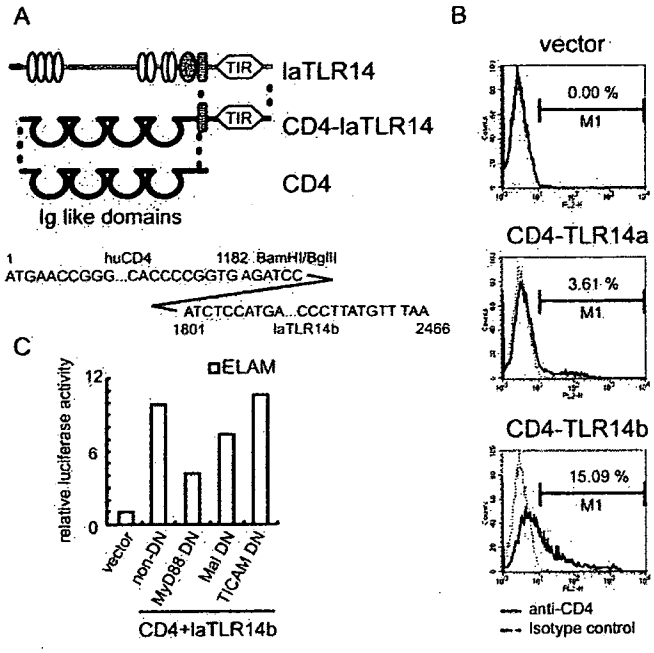

FIGURE 5. laTLR14b activates NF-κB via MyD88 in human cells. *A*, Constructions of constitutive active forms of laTLR14a (CD4-TLR14a) and laTLR14b (CD4-TLR14b). The sequence of fused cDNAs extracellular domains of human CD4 and each TIR domain of laTLRs is shown. *B*, Expression of the fused proteins in HEK293 cells. Twenty-four hours after transfection of the indicated cDNAs into HEK293 cells, the protein expression levels of CD4-TLR14a and 14b on the cell surface were measured by flow cytometry using anti-CD4 Ab conjugated with PE. Protein expression is barely detectable in cells transfected with the empty vector (*top*) or CD4-TLR14a cDNA (*center*). Only CD4-TLR14b expression is detectable on the surface (*bottom*). *C*, Luciferase reporter assay was performed to measure the levels of activation of NF-κB. An empty vector and each CD4-TLR14 construct were transfected into HEK293 cells together with an ELAM-luciferase reporter plasmid. The dominant negative (DN) forms of MyD88 (MyD88 DN), Mal/TIRAP (Mal DN), or TICAM-1 (TICAM DN) were simultaneously expressed in HEK293 cells in addition to the above proteins as described in the *Materials and Methods*. After 24 h, luciferase activities in cell lysates were measured. Relative luciferase activities are shown as described previously for determination of activation of NF-κB (26). Experiments were performed in triplicate. Results of one of the three experiments is shown.

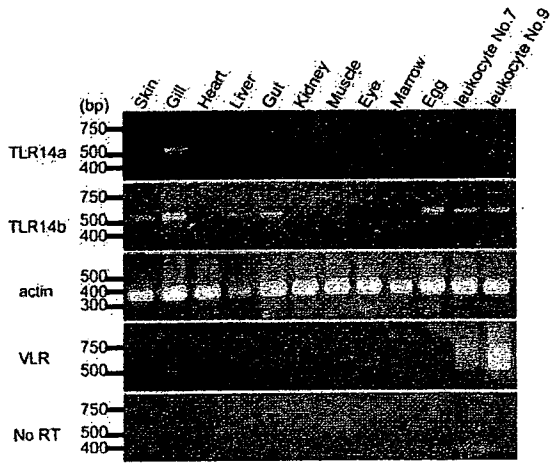

FIGURE 6. Tissue distribution of laTLR14a/b in comparison with VLR. Tissue distribution of mRNA of laTLRs in *L. japonica* organs. Amplifications of TLR gene fragments were accomplished by the RT-PCR technique using equal numbers of PCR cycles. Cytoskeletal actin (actin) of lamprey was used for a positive control, and templates without reverse transcriptase (no RT) were used for a negative control. The control PCRs were performed with all of the primer sets indicated in the figure and no band was detected (data not shown). Results using the actin primers are shown here. cDNAs were prepared from total RNA in each tissue from 13 individual lampreys. The conditions of the PCR analysis are described in the *Materials and Methods*. Amplified DNA fragments were electrophoresed in 1% agarose gel and visualized by ethidium bromide staining. A representative mRNA distribution profile obtained by PCR analysis is shown here because similar results were obtained with each individual regarding the laTLR14a/b distribution profiles. VLR is exclusively expressed in lamprey leukocytes, but the VLR mRNA levels appear to be different among individuals. Examples are shown with leukocytes (animals no. 7 and no. 9).

Comparison of laTLRs with VLR

Distribution of laTLR14a and 14b were determined by RT-RCR using cDNAs from various tissues as templates. For this purpose, lampreys were harvested in the Ishikari river every winter for 5 years. Individual lamprey showed similar laTLR14a/b mRNA expression profiles (Fig. 6). laTLR14a mRNA was exclusively expressed in the gills of lampreys. In contrast, laTLR14b mRNA was expressed in the skin, gills, heart, liver, gut, and leukocytes (Fig. 6). The strongest signal was obtained in the gill and gut. We could not confirm the results by immunoblotting or histochemical staining using the anti-laTLR14b Ab (data not shown), which may reflect the low protein expression levels of this protein in various organs.

It has been reported that lampreys express proteins with various sets of tandemly arranged LRRs named VLRs in their lymphocyte-like cells and that VLRs are related to the lamprey immune system (12, 13). We isolated these cells as described earlier (11), extracted RNA, and confirmed the existence of VLR messages using RT-PCR (Fig. 6). The VLR mRNAs were unequivocally detected in leukocytes but too faint to see in other organs by ethidium bromide staining. The VLR mRNA bands were detectable in the organs including the gill, heart, and gut after repetitive PCR (data not shown). It is likely that the origin of the VLR mRNAs is blood leukocytes. The results showed that leukocytes express both laTLR14b and VLR. Based on the broad PCR bands corresponding to VLR, its primary sequences appeared to be variable. To determine actual nucleotide sequences of the VLRs, we cloned the PCR amplicons and sequenced. The alignment of the representative amino acid sequences is shown in Fig. 7*A*. In contrast, laTLR14b from the same individual did not show such high rates of variation or heterogeneity in their sequences (Fig. 7*B*). The sequence invariability of laTLR14b was confirmed with four individual lampreys harvested in different years (data not shown). The single amino acid substitutions were observed in the sequences of laTLR14b, probably due to artifacts of polymerase misreading. Hence, the heterogeneity occurs selectively in VLRs but not in TLRs in lampreys. The lamprey TLRs, at least TLR14a and 14b, evolved independently of the VLR family, resulting in the formation of a distinct LRR system with differential functions.

Discussion

In this study, we demonstrated the following. First, the lamprey possesses type I membrane proteins consisting of LRRs and the TIR domain that may be classified into the TLR family based on their structure. We call these proteins laTLR14a and laTLR14b. Second, the localization analysis in human and fish cell lines revealed that the lamprey TLR-like proteins largely reside in the cytoplasmic compartment ER in human cells. In transfected fish cell lines, the laTLR14s were localized to the ER and other organelles.

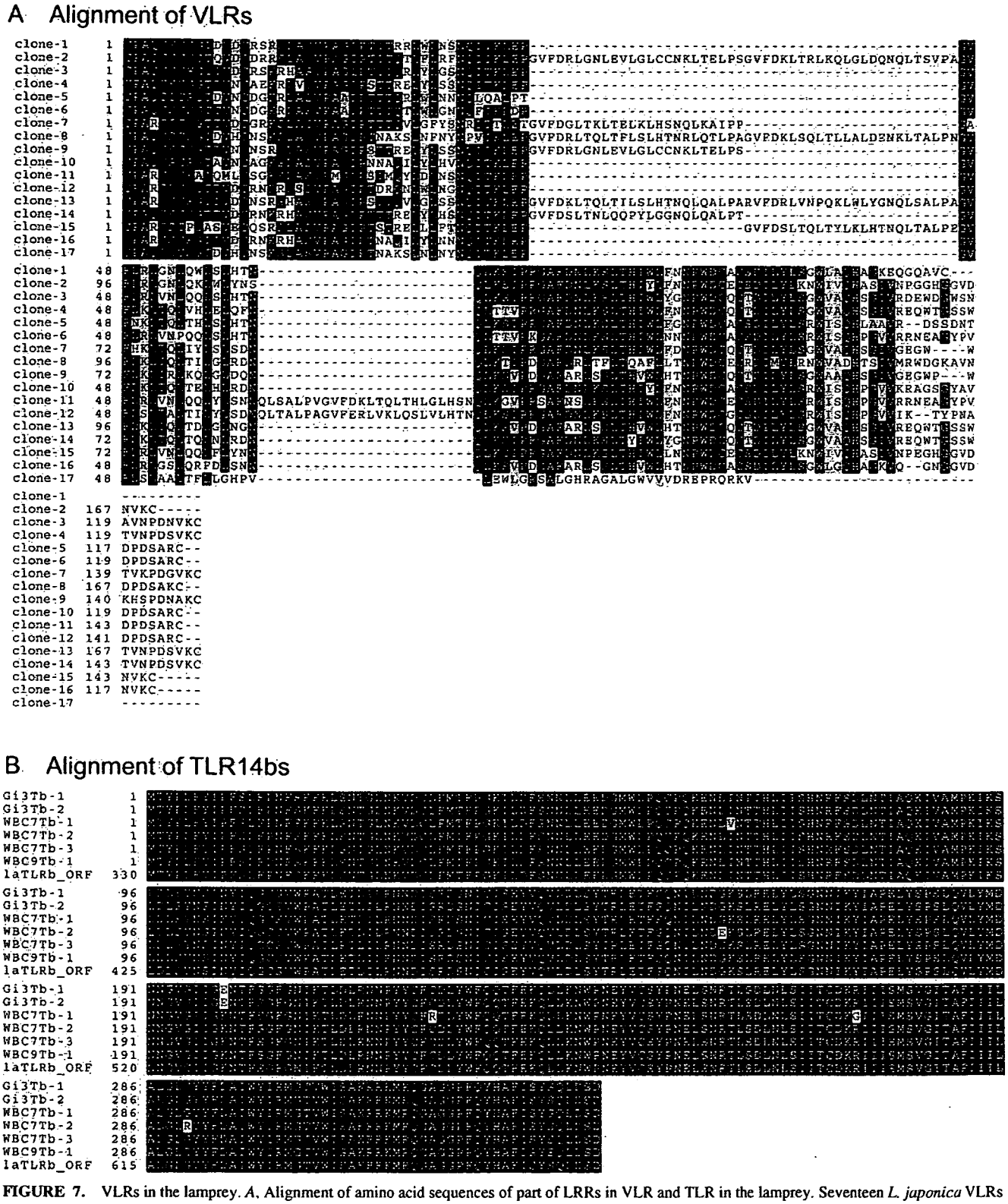

FIGURE 7. VLRs in the lamprey. *A*, Alignment of amino acid sequences of part of LRRs in VLR and TLR in the lamprey. Seventeen *L. japonica* VLRs were cloned from the mRNA of gill (animals no. 1 to no. 5), gut (animals no. 6 to no. 10) and leukocytes (animals no. 11 to no. 17). The VLR clones may be originated from blood leukocytes. laTLR14b DNA fragments were cloned from cDNA libraries of three individual fish (animals no. 3, no. 7, and no. 9) *B*, Gi, gill; WBC, white blood cells. The cloned laTLR14b fragments did not exhibit any diversity like VLRs. The identical residues are shaded by BOXSHADE program (www.ch.embnet.org/software/BOX_form.html).

Third, NF-κB and IFN-β promoter activation was promoted in human cells by artificial dimerization of the lamprey protein laTLR14b. Fourth, Lamprey TLR proteins existed structurally independent of VLR; these TLR proteins were neither variable in their primary sequences nor expected to have GPI anchors. Fifth, laTLR14b was preferentially expressed in the gills, gut, and leukocytes. Thus, the lamprey most likely has immune-related TLRs structurally distinguished from the reported VLR proteins. In TLRs, the LRR motif serves to